KEMIAN LAITOS
JYVÄSKYLÄN YLIOPISTO

Multicomponent peptide-based hydrogels

M. Sc. thesis

University of Jyväskylä

Department of Chemistry

17.1.2024

Tiitta Rouhiainen

Abstract

The literature part of this master's thesis focuses on multicomponent supramolecular gels. Multicomponent self-assembly leads to the formation of highly organized and complex structures, providing the opportunity to generate properties to hydrogels that cannot be achieved with single-component gels. The thesis explored the properties, design, characterization, and biomedical applications of multicomponent gels, with a specific focus on peptide-based ones.

The experimental part of the thesis investigated the formation and structure of a two-component hydrogel comprising Fmoc-F and Fmoc-L. The participation of Fmoc-L in gel formation was explored using ^{1}H NMR and fluorescence spectroscopy. FTIR spectroscopy was used to analyze the secondary structures of the gels and phase transition temperatures ($T_{gel\text{-}sol}$) were measured to detect potential macroscopic differences among gels prepared using varying ratios of the gelators. Furthermore, AFM imaging was performed to find an optimal sample preparation protocol for future sSNOM experiments.

Tiivistelmä

Tämän pro gradu -tutkielman kirjallisuusosa käsittelee monikomponenttisia supramolekulaarisia geelejä. Monikomponenttinen itsejärjestäytyminen johtaa erittäin järjestäytyneiden ja monimutkaisten rakenteiden muodostumiseen sekä tarjoaa mahdollisuuden aikaansaada ominaisuuksia, joita ei voida saavuttaa yksikomponenttisilla geeleillä. Tutkielmassa perehdyttiin monikomponenttigeelien ominaisuuksiin, suunnitteluun ja karakterisointiin sekä biolääketieteellisiin sovelluksiin, keskittyen erityisesti peptidipohjaisiin monikomponenttigeeleihin.

Tutkielman kokeellisessa osassa tutkittiin Fmoc-F:a ja Fmoc-L:a sisältävän kaksikomponenttihydrogeelin muodostumista ja rakennetta. Fmoc-L:n osallistumista geelin muodostumiseen tutkittiin ^{1}H NMR-spektroskopialla ja fluoresenssimittauksilla. Geelin sekundaarirakenteiden tutkimiseen käytettiin FTIR-spektroskopiaa. Faasimuutoslämpötilat ($T_{gel\text{-}sol}$) mitattiin mahdollisten makroskooppisten erojen havaitsemiseksi eri ainemääräsuhteilla valmistettujen geelien välillä. Lisäksi otettiin AFM-kuvia sopivan näytteen valmistusmenetelmän määrittämiseksi tulevia sSNOM tutkimuksia varten.

Preface

The experimental part of this master's thesis was carried out between January 2023 and May 2023 at the Nanoscience Center of the University of Jyväskylä. The literature part of the thesis was done from May to December in 2023. Literature sources were searched through Google Scholar and Web of Science databases. The thesis was supervised by Professor Maija Nissinen, and the experimental work was supervised by M. Sc. Romain Chevigny. I would like to thank both of them for their excellent guidance and assistance throughout the work.

Contents

Abbreviations

A	Adenine
ACN	Acetonitrile
Aeg	N-(2-aminoethyl)-glycine
AFM	Atomic force microscopy
APIs	Active pharmaceutical ingredients
C	Cytosine
CD	Circular dichroism
C14	Myristyol
DOPA	Dihydroxyphenylalanine
GFFY	Gly-Phe-Phe-Tyr
ECM	Extracellular matrix
F/Phe	Phenylalanine
FF	Diphenylalanine
FEG-SEM	Field Emission Gun-Scanning Electron Microscopy
Fmoc	9-fluorenylmethyloxycarbonyl
FT-IR	Fourier-Transform Infrared spectroscopy
G	Guanine
GA	Glucuronic acid
GdL	Glucono-δ-lacton
HAP	Hydroxyapatite
IFE	Inner Filter Effect
KGM	Konjac glucomannan
L	Leucine

LMWG	Low molecular weight gelator
MGC	Minimum gel concentration
NAG	N-acetyl glucosamine
NDI	Naphtalenediimide
OPV	Oligo(p-phenylenevinylene)
OT4	Quarterthiophene
PBI	Perylenebisamide
PBS	Phosphate-buffered saline
PNA	Peptide nucleic acid
PTZ	Phenothiazine
R	Arginine
RET	Resonance energy transfer
SAS	Small angle scattering
SANS	Small angle neutron scattering
SAXS	Small angle X-ray scattering
SEM	Scanning Electron Microscopy
SPPS	Solid-phase peptide synthesis
SSG	Self-supporting hydrogel
sSNOM	Scattering scanning near-field optical microscope
T	Thymine
Tyr	Tyrosine
TEM	Transmission Electron Microscopy
USANS	Ultra small angle neutron scattering
UV-vis	UV-visible spectroscopy

LITERATURE PART

1 Introduction

Low-molecular-weight supramolecular gels are composed of small molecules known as gelators, which, in a suitable solvent, assemble into nano- or microscale network structures forming the gel.[1] Noncovalent interactions maintain the network structure and induce the self-assembly of LMWGs.[2] The typical composition of supramolecular gels involves two components: the solvent and the gelator. Multicomponent supramolecular gels can be prepared by introducing more than one compound into the solvent. These multicomponent gels provide a convenient way to tailor gel properties, such as by altering the ratio of components. The most extensively studied to date are the simplest multicomponent gels, which consist of the addition of two components to the solvent.[1]

Since many artificial nanostructures consist of a single class of building blocks, the level of functional and structural complexity, tunability and diversity is limited. However, through multicomponent self-assembly, there exists an opportunity to create more complex structures, enhancing modularity and enabling self-assembly with spatiotemporal control. By employing two or more distinct building blocks interactions such as, protein-peptide, protein-protein, peptide-peptide, PA-polysaccharide, and protein/protein-DNA, leveraging the synergistic properties of these multicomponent molecules, the performance and structure created from these systems can offer new possibilities for more functional and intricate material design for applications such as tissue engineering, drug delivery, the design of nanoreactors, and optoelectronics.[3,4]

Nature is full of highly functional, complex and synergistic protein-based multicomponent assemblies. Taking inspiration from nature, utilizing multicomponent self-assembly has emerged as a platform for creating highly organized, dynamic, and complex nanostructures based on proteins and peptides. Peptides and proteins serve as sources of inspiration for new molecules, assembly mechanisms and as resources of versatile building blocks. The aim is also to decode the encoded information within proteins to create design rules for the development

of smart materials.[5] As self-assembly is relies on non-covalent interactions, engineered self-assembling peptides have the potential to act as building blocks for gel scaffolds, addressing immunogenicity concerns and achieving biocompatibility. Other advantages include relatively low-cost production, simple synthesis, potential chemical modifications, and potential *in situ* organization.[6]

2 Supramolecular gels

Generally, gels have been characterized by their covalently cross-linked polymer networks. However, supramolecular gels rely on noncovalent interactions for self-assembling into hierarchical structures, challenging this framework.[7] Supramolecular gels utilize noncovalent interactions to form three-dimensional (3D) entangled network structures. These structures contain a large amount of entrapped solvents, such as water in hydrogels and other solvents in organogels).[7,8] Depending on the framework of the network, supramolecular gels can be divided into two categories: polymeric or molecular gels. Supramolecular polymeric gels (Figure 1a) consist of polymer backbones along with additional noncovalent interactions. Noncovalent interactions enhance the number of cross-linking points within the gel structure. In contrast, the backbone of molecular gels (Figure 1b) is formed by the self-assembly of low-molecular-weight gelators (LMWGs). Noncovalent interactions, such as hydrogen bonding, π-π stacking, and metal-ligand interactions, are responsible for maintaining the network structure.[9]

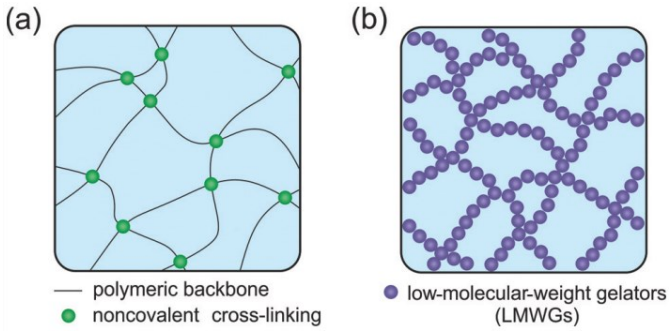

Figure 1. a) Supramolecular polymeric gel and b) supramolecular LMWG gel.[9] Reprinted with permission from ref. 6., Copyright 2021 Organic Materials.

The gelation process of LMWGs is very dynamic. Initially, gelators are dissolved in a state of "high solubility", achieved by, e.g., higher temperature or a favorable solvent. The hierarchical self-assembly of supramolecular gels occurs when conditions, such as a decrease in temperature, transition them into a "low solubility" state. Gelators nucleate and self-assemble along one dimension, forming nanofibrils that frequently aggregate into bundles of fibrils. As these nanofibers gain a specific length, they entangle, resulting in the formation of solid-like network and gelation (Figure 2).[9,10]

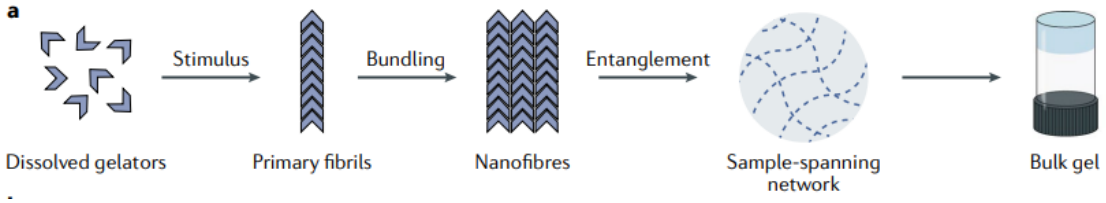

Figure 2. Hierarchical self-assembly of low-molecular-weight gelators (LMWGs) occurs due to the influence of an appropriate stimulus, causing individual gelator molecules to assemble through noncovalent interactions, forming fibrils. These fibrils bundle together to form wider nanofibers, and their entanglement leads to the formation of a solid-like network and gelation.[10] Reprinted with permission from ref. 7., Copyright 2019 Springer Nature.

Since noncovalent interactions, such as hydrophobic interactions, van der Waals interactions, hydrogen bonding, π-π stacking, charge-transfer interactions, etc., maintain the network, the self-assembled gels respond well to stimuli such as pH, heat, UV-light and ionic analytes, making them exceptionally dynamic. Because of this responsive behavior, materials with very different properties can be prepared.[3,8] To expand the functionalities and applications of supramolecular gels, there is increasing exploration of using multiple LMWGs to create more complex systems.[9]

2.1 Multicomponent supramolecular gels

Gel properties can be modified by incorporating two or more components during self-assembly.[3] In this way, it is possible to adapt the properties of the gel, e.g. by changing the proportions of the different components.[1] Multicomponent systems like this are interesting because of their remarkable advantages over single-component systems and because of their many applications.[3]

Multicomponent self-assembly opens possibilities for creating materials with adjustable mechanical properties, and various morphologies. Several systems have been reported in which certain properties of the mixture have improved compared to their individual components. Examples of advantages include self-replication, enhanced intrinsic fluorescence, strong mechanical properties, resistance to high yield strain, efficient DNA binding and tumor suppression, enhanced tunability of properties, high stability, and efficient energy transfer. The reasons for such improvements in properties are not always fully understood. The improved structures and properties that emerge from these systems offer new ways of designing more complex functional materials.[11,12]

2.2 Multicomponent self-assembly in nature

Nature provides valuable insights into multicomponent self-assembly. Biological structures such as phospholipid cell walls and DNA exhibit remarkable structural and functional complexity, which arises from their capacity to assemble a wide range of building blocks into defined constructs. During this process, small or large molecules come together individually or cooperatively, creating biomaterials with diverse functions. The functionality of these and numerous other biological structures is achieved from their ability to form highly ordered structures, the inherent properties of their components, and their interactions, offering adaptability, dynamism, and responsiveness. There are examples of this in several biological structures, such as the strong and dynamic structures created by actin and myosin or the significant firmness of silk arising from interactions between sericin and fibroin. In contrast to

biologically encoded molecular tissues, non-biological self-assembly in multicomponent systems is typically built through a complicated pathway. The complexity of self-assembly depends on factors like the component interactions, surrounding environment, and structural similarities among the components.[4,5]

Taking inspiration from these examples, efforts have been made to develop materials in which proteins and peptides are utilized as multicomponent ensembles, unveiling new properties through their interactions.[5]

2.3 Gelation of multicomponent supramolecular gels

The gelation of individual molecules is a multi-level self-assembly process. The process starts with phase separation, leading the molecules to self-assemble into one-dimensional fibers. A hydrogel network is formed when these fibers become entangled or cross-linked. When two or more components are present, phase separation occurs independently or together. Self-sorted gel networks are formed by the independent phase separation of the components. In such a gel network, the pure assemblies of one component coexist alongside the pure assemblies of another component. On the contrary, individual fibers containing both components are formed through co-assembly. Several factors, such as steric effects, chirality, complementarity of hydrogen bonds, thermodynamic and kinetic pathway control, etc., affect which way the assembly takes place. It is also possible that both self-sorting and co-assembly and self-sorting occur simultaneously.[3] Three general categories of multicomponent supramolecular gels have been studied (Figure 3).[1]

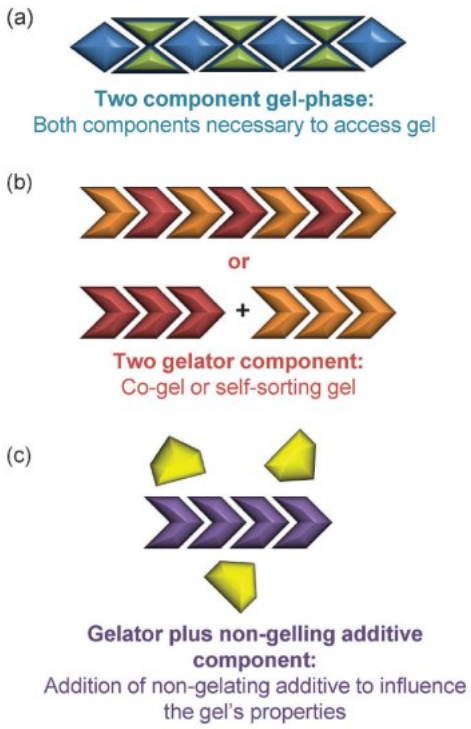

Figure 3. Three main types of multicomponent supramolecular gels.[1] Used with permission of RSC, from Supramolecular gels formed from multi-component low molecular weight species, Buerkle, L. E. and Rowan, S. J., 41, 2012; permission conveyed through Copyright Clearance Center, Inc.

In the first type, none of the components form a gel independently. Gelation requires all the components to form a gel. Gelation mainly occurs through hydrogen bonding, donor-acceptor or metal-ligand interactions.[1] In the case of two-component gels, self-assembly occurs through the formation of a complex. Two separate, complementary components initially form a complex, which then self-assembles into a fibrous supramolecular polymer (Figure 4). The formation of the complex before fibrillar assembly introduces an extra level of control within the hierarchical self-assembly process, as well as excellent tunability and control. The behavior and the morphology of the two-component materials can be altered by making structural changes to either of the components or by adjusting the ratio between the components.[13]

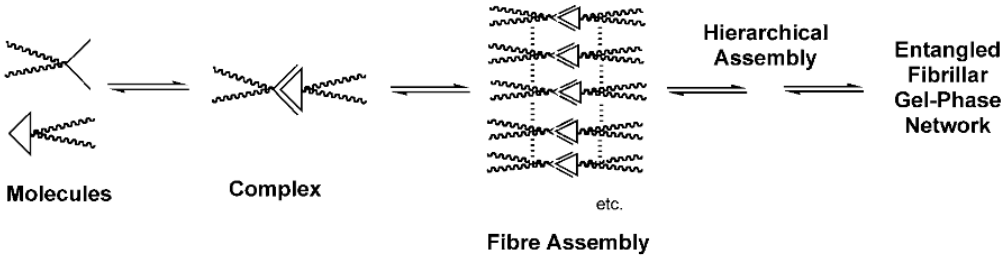

Figure 4. Formation of a complex and self-assembly of a two-component gel-phase material.[13] Reprinted with permission from ref. 12., Copyright 2005 John Wiley & Sons, Inc.

The second category uses two or more gelators that can either self-sort or co-assemble into separate assemblies.[1] If both components are gelators, several possible types of fibrous networks can be formed.[14] Self-sorting can occur, where two LMWGs prefer self-assembly with each other, resulting in self-assembled structures composed exclusively of one LMWG. Self-assembly can also occur in such a way that there are strong interactions between the two gelators, resulting in co-assembled structures with alternating gelators. Lastly, LMWGs can non-specifically mix, yielding randomly mixed self-assembled structures. Formed fibers can interact through entanglements or form two completely independent, interpenetrating gel networks (Figure 5).[15,16]

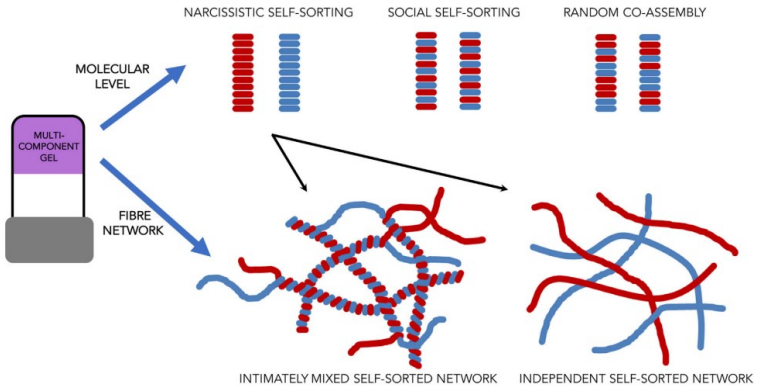

Figure 5. When both molecules are independently capable of forming fibers, combining these molecules in mixed systems can produce different results at the molecular level (top). The properties of the gel are closely related to the primary level of assembly and the subsequent hierarchical arrangement. For instance, on hierarchical level, self-sorted fibers can intricately entangle or form an interpenetrating network (bottom).[15] Reprinted with permission from ref. 14., Copyright 2017 from Elsevier.

It is also possible that the assembly of the two gelators occurs with varying degrees of self-sorting and co-assembly. It can be assumed that if the co-gelators have similar binding motifs, they prefer mixed configurations, and if the binding motifs are very different, they show a thermodynamic preference for self-sorting.[1] If one system forms gel networks before the other, this affects the later self-assembly. If gelators do not co-assemble, it is still possible that one component influences the assembly of the other system.[14]

The last category comprises one or more gelators and one or more non-gelling additives that can affect the gel assembly process and, thereby, the properties of the gel.[1] Non-gelling additives can be used to modify thermal or mechanical properties, add additional functional properties or improve the stability of the gel.[1] In these systems, the self-sorting of the gelator leads to forming of the gel matrix, while the additive significantly affects the nucleation and growth of the fibers and consequently regulates the bulk properties of the gel. If the gelator and the non-gelling additive have similar molecular structures, it is also possible that their mixture leads to co-assembly.[3]

Predicting the state of self-assembly of a multicomponent system could enable better control of the structure and properties of the gel, but this has proven to be very difficult. Firstly, minor changes in the structure of the gelator affect the properties of the gel, and additionally, controlling interactions among individual gelators on a molecular level presents a significant challenge.[17]

4 Peptides and amino acids as gelators

Amino acids and peptides are organic compounds that exhibit characteristics of low molecular weight gelators. They tend to self-assemble through low energy interactions, such as hydrophobic affinity, van der Waals and electrostatic forces, hydrogen bonds, and π-π interactions.[18,19]

Due to their high modularity with respect to order (i.e., nature (e.g., basic, acidic, aliphatic, aromatic,), number and position of the amino acids), peptides are great candidates to design soft materials.[19] Supramolecular gels based on peptides and amino acids are very important in

biomedical applications due to their inherent properties like cellular adhesion, bioactivity, biocompatibility and proliferation. Peptide-based gels are used, e.g. in controlled release of bio-active compounds (e.g. antibiotics, mRNA, growth factors, LgG), in wound dressings with antibacterial and repairing effects, tissue engineering, adjuvants for vaccines and MRI imaging.[18,19]

External factors such as pH changes, temperature, solvent polarity, and alteration of ionic strength can trigger the gelation process. As a result of these factors, various secondary structural arrangements, such as β-sheet, α-helix, and β-hairpin, are formed. They depend on the inter- and intramolecular bonds formed between amino acid residues. π-π interactions of aromatic moieties between two peptides play a significant role in the self-assembly processes leading to β-sheet structures.[18]

4.1 Diphenylalanine (FF) and Fmoc

Diphenylalanine (FF; **1**) and its derivatives are widely recognized as the basic peptide building blocks in the fabrication of self-assembling materials. FF (Figure 6) represents the minimal segment of the Alzheimer's disease Aβ peptide that exhibits spontaneous self-assembly. Supramolecular assemblies derived from FF frequently exhibit distinct properties compared to the native dipeptide, significantly broadening the potential applications of the resulting materials.[20] Diphenylalanine has found applications in various fields, ranging from semiconductor nanophotonics to optics. However, one of the most popular applications of the diphenylalanine motif has been its incorporation into short peptides that form hydrogels. These self-assembling peptide hydrogels incorporating diphenylalanine are “capped” with an aromatic group at their N-terminus. The selection of this protection group significantly influences the subsequent peptide self-assembly.[21]

It is well-documented that the diphenylalanine sequence alone does not possess the capability to form hydrogels but instead tends to form crystalline nanotubes. However, if 9-fluorenylmethyloxycarbonyl (Fmoc; **2**) is attached to the N-terminus of the diphenylalanine sequence, it forms a self-supporting hydrogel.[21] Fmoc (Figure 6) is a voluminous aromatic

group used as a base sensitive protection group to amino acids and short peptides and at the N-terminal. Its aromatic rings plays a significant role in terms of physicochemical properties when they arrange themselves to form structures via π-π stacking.[18]

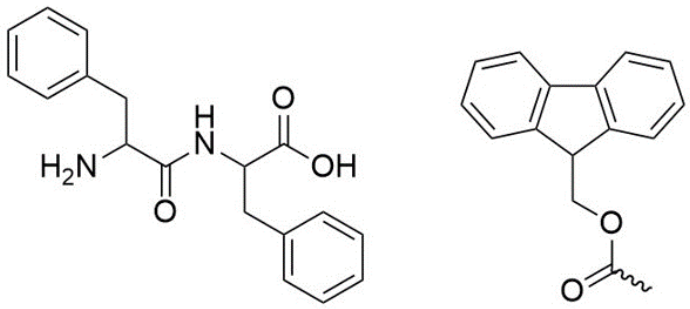

1 **2**

Figure 6. Molecular structures of diphenylalanine (FF; **1**) and 9-fluorenylmethoxycarbonyl (Fmoc; **2**).

Fmoc-FF is one of the most widely used examples of LMWGs. Fmoc-FF, utilizing the β-sheet motif, self-assembles into a fibrous hydrogel network under physiological conditions without a cross-linking reaction.[6,22] The ease of synthesis is also one of the factors for the popularity of Fmoc-FF in various applications. Fmoc-FF can be synthesized using either solution or solid-phase peptide synthesis (SPPS) methods, and it is also commercially available.[21] Combining Fmoc-FF with other molecular entities enables the design and fabrication on entirely new, multicomponent nanomaterials with diverse properties.[22]

4.1 Peptide-based multicomponent hydrogels

Peptide-based biomaterials are biologically compatible materials with countless modification possibilities and the ability to self-assemble into hydrogels mimicking the structural composition of the extracellular matrix (ECM). Therefore, they have numerous applications in

biomedicine. The synthesis of peptide materials follows a bottom-up approach using the 20 standard proteogenic amino acids, each with varying molecular properties. In biomaterial research, there is an increasing interest in self-assembling peptides due to their properties, such as biological diversity and chemical versatility. Secondary interactions of molecules combined with peptide secondary structures (e.g., α-helices, β-turns, β-strands, coiled coils and random coils) offer numerous opportunities to direct self-assembly and development of new structures.[23]

To introduce new properties and optimize the material, diverse alterations have been made to the peptide sequences. These modifications include, for example, the integration of aliphatic chains, large aromatic moieties (e.g., naphthyl, Fmoc), halogen atoms, and pseudopeptic bonds. Also, the advancement of peptide-based hydrogels composed of multiple gelators emerges as a promising approach to overcome some inherent limitations associated with single component peptide-based hydrogels. However, designing and characterizing multicomponent peptide-based hydrogels can be challenging due to the diverse co-assemblies that peptide derivatives can form, and predicting their properties is difficult, limiting their potential. Hence, they are still limited to a few instances employing five primary strategies.[19]

The first approach involves fabricating hydrogels by combining self-assembling peptide with the same peptide modified with biological recognition motifs, introducing novel functional features (peptide[A] + peptide[A] functionalized with biologically relevant motifs). The second strategy includes the mixing of self-assembling peptides with longer peptides, consisting of two sequences of the same peptide linked by a spacer (peptide[A] + peptide[A]-linker-peptide[A]). This enhances cross-linking between fibrils. The third strategy, the most widely studied one, involves the creation of multicomponent peptide-based gel using short peptides with N-terminal protection by a Fmoc moiety (Fmoc-peptide[A] + (Fmoc)-peptide[B]). In the fourth approach, the utilization of D-peptides in combination with native peptides and L-amino acids (enantiomeric peptide mixtures) has been proposed. The fifth strategy centers around the formation of multicomponent peptide-based hydrogels through the co-assembly of oppositely charged peptides facilitated by, e.g., the formation of ion pairs (oppositely charged peptides).[19]

Stefan and his research group[24] investigated six multicomponent hydrogels formed from a mixture of heptapeptides that were N-terminally functionalized with one peptide nucleic acid. The study used five compounds built from a heptapeptide H_2N-Glu-(Phe-Glu)$_1$-(Phe-Lys)$_2$-OH (**3**), derived from an octapeptide H_2N-Phe-Glu)$_2$-(Phe-Lys)$_2$-OH. To add nucleobases, the

peptide was N-terminally functionalized with peptide nucleic acids (PNA).[19] PNA is a nucleic acid analogue in which a synthetic peptide backbone, usually composed of N-(2-aminoethyl)-glycine units (Aeg), has replaced the sugar phosphate backbone of natural nucleic acid. It is not expected to degrade in living cells, as it is resistant to enzymatic cleavage and chemically stable.[24]

The five compounds in the study were PNA(X)-pep, where X = adenine (A; **4**), thymine (T; **5**), cytosine (C; **6**) or guanine (G; **7**), and nucleobase-lacking equivalent Aeg-pep (**8**) for comparison. In the multicomponent mixtures, there were two compounds present in an equimolar amount (1:1), with a total concentration of 15 mM. Thus, all samples contained 7.5 mM of each peptide derivative.

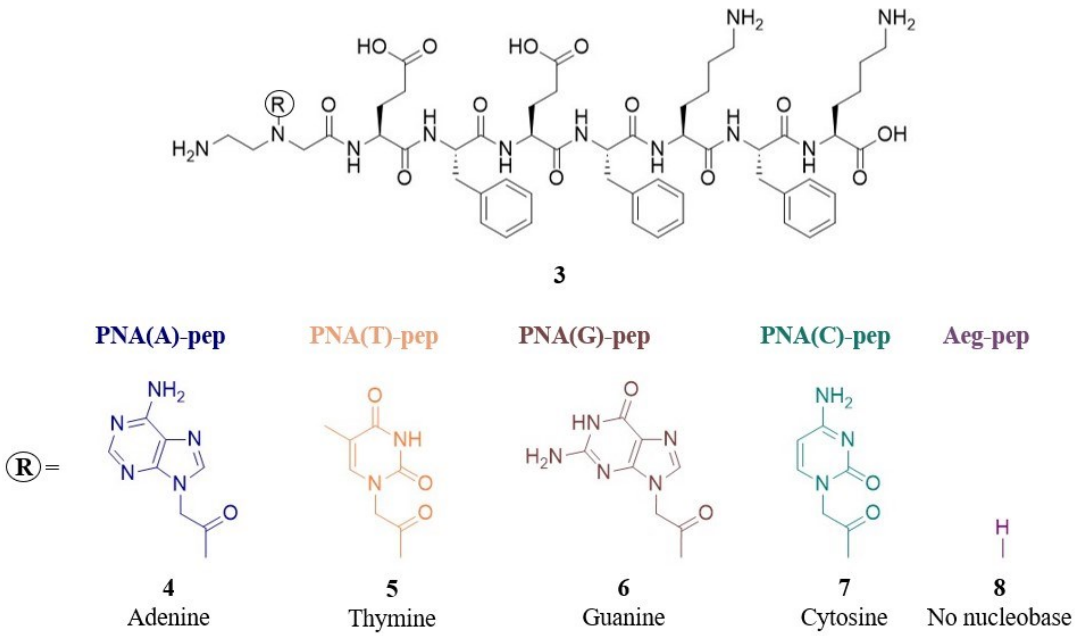

Figure 7. Structural compositions of hybrid DNA nucleobase/peptide derivatives and DNA-nucleobase-lacking peptide (Aeg-pep).

Two of the combinations (PNA(A)-pep + PNA(T)-pep and PNA(G)-pep + PNA(C)-pep) formed translucent gels and three of the combinations (PNA(A)-pep + Aeg-pep, PNA(T)-pep + Aeg-pep and PNA(G)-pep + Aeg-pep) formed clear gels. PNA(C)-pep + Aeg-pep didn't form a gel (Figure 8). The hydrogels that exhibited the highest rigidity and fastest formation were

achieved from two multicomponent mixtures comprising pairs of complementary DNA-nucleobases (i.e., adenine + thymine and guanine + cytosine). The synergistic effect arising from the presence of these two complementary nucleobases in the co-assembly process affects structural (morphology of the nanoobjects), mechanical (stress resistance and stiffness and stress), and physicochemical (fluorescence properties, kinetics of formation) properties. The mechanical and kinetic properties of other mixtures with Aeg-pep appear to be influenced by the PNA(X)-pep (X=A, T, C, G) component. Their sol/gel transition times ($t_{s/g}$), storage moduli, compactness, resistance to stress (τ_y), and ability to constrain the solvent follow the same trend as observed for hydrogels prepared from PNA(X)-pep alone, which is G- > A- > T- > C-containing nucleopeptide. This is partly due to stronger π-stacking interactions between the purines G and A compared to the pyrimidines C and T.[19]

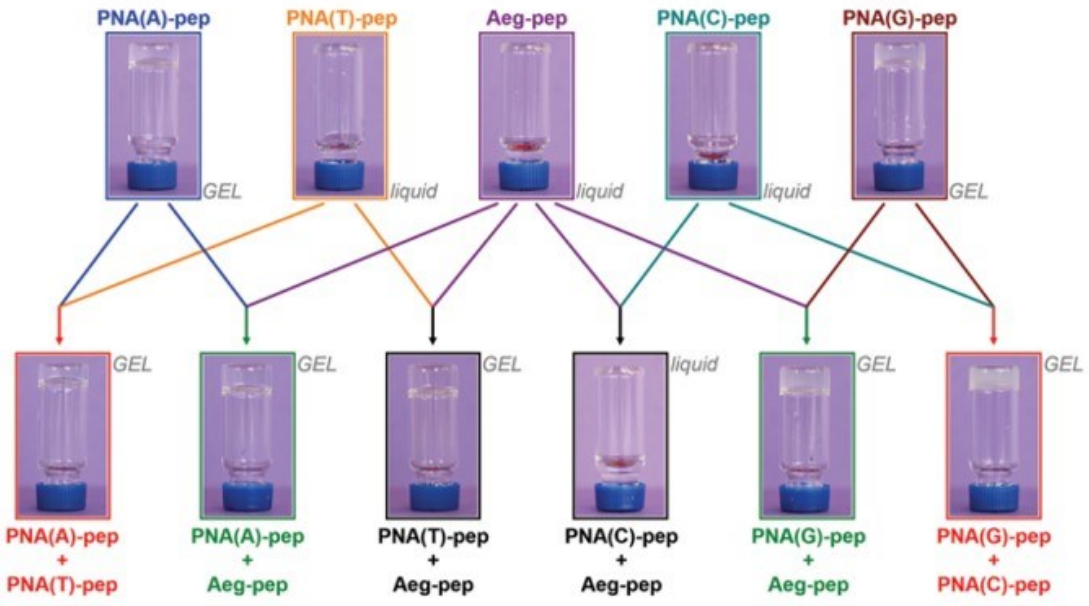

Figure 8. Images of all mixtures showing the formation (or lack of formation) of hydrogels. The main focus of the study was on six equimolar multicomponent mixtures, shown at the bottom.[19] Reproduced and adapted from ref. 18., Copyright 2020 with permission from the Royal Society of Chemistry.

The research outlines the complexity of studying and comprehending these complicated supramolecular assemblies. Given practically unlimited possibilities for designing peptide

derivatives, altering the number of constituents, or adjusting the equivalent ratio between each component, multicomponent physical hydrogels present fresh application opportunities, allowing enhanced control over mechanical and physicochemical properties.[19]

5 Designing multicomponent gels

Despite extensive research on LMWGs, their precise design rules are not fully understood. Small differences in assembly conditions and molecular structure can determine the distinction between a gelator and a non-gelator. Therefore, a complete understanding of the gelation process is challenging and becomes even more complex in systems involving multiple gelators. The complexity increases due the need to comprehend how two LMWGs interact in each other's presence.[25]

In order to synthesize gelators with targeted properties, it would be crucial to establish some kind of design guideline to prepare LMWGs that produce predictable properties.[17] Some research has attempted to recognize connections between molecular structure and gelation, such as solvents and terminal groups, but there are hardly any examples of a multicomponent gelator system that has been intentionally designed and systematically explained.[17,25]

When designing multicomponent systems, it is possible to assume that self-sorting occurs if the components forming the gel have very different structural motifs, while structural similarity leads to co-assembly.[25]

5.1 Structural similarity

In the design of multicomponent systems comprising gelators with similar structures, a fairly simple approach is to use enantiomers. Chirality is a phenomenon that occurs everywhere in nature, from molecular-level L-amino acids and nanoscale helices to macroscopic assemblies. Supramolecular chirality, emerging from the asymmetric spatial arrangement of the components in assemblies formed through noncovalent interactions, is closely linked to the chirality of the molecular components and the way they are assembled, making it a reasonable approach to consider when designing co-assembling multicomponent LMWG systems.[25–27]

It has been reported that Individual enantiomers exhibit better gelation properties (individually) in comparison to racemic mixtures. Racemates often lead to precipitation; thus, gelation does not occur. Enantiomers, on the other hand, form aggregates, followed by the growth of fibrils, then the formation of the network and eventually gelation. However, racemic mixtures can, in some cases, form gels through the conglomerate formation. Conglomerates break down into separate aggregates, resulting in gelation.[25]

When supramolecular gels based on enantiomers are mixed, the gel fibers rearrange at the molecular level, resulting in tunable properties and improved packing. Tómasson *et al.*[28] synthesized bis(urea) compounds labelled with phenylalanine methyl ester in racemic and enantiopure forms. Both enantiopure and racemic compounds formed gels in several solvents. The gels were characterized using standard gelation analysis techniques (gelation test using vial inversion, minimum gel concentration (MGC), gel-to-solution transition temperature (T_{gel}) and frequency sweep experiments to study rheological properties) and AFM, SEM and solid-state NMR were used to examine the morphology of the gels. Circular Dichroism (CD) was used to provide information about molecular chirality.[28]

Racemate (1-rac) formed a more robust gel network in comparison to enantiomers. However, the gel (1R+1S), produced by combining equimolar quantities of enantiomers (1R and 1R), indicated the best thermal and mechanical stabilities in comparison to both enantiomers and racemate gels (Figure 9). The preservation of chirality on the gel fibers was demonstrated using CD. Gels composed of enantiopure compounds exhibited helical fibers, while racemate exhibited tape-like structures, suggesting the co-assembly of individual enantiomers. The analysis of AFM and SEM images, along with solid-state NMR, unveiled that the network

within the mixed gel comprises a combination of enantiomeric and racemate fibers. The presence of both co-assembled and self-sorted fibers in the mixed gel was confirmed by solid-state NMR through the analysis of xerogel packing and the observation of twisted-tape morphology in AFM and SEM images. This observation suggests that in mixed gel system, fibers reorganize to form both co-assembled and self-sorted fibers. The simultaneous presence of co-assembled and self-sorted fibers can be considered to cause the improved thermal stability and mechanical properties compared to the enantiomer and racemate gel.[28]

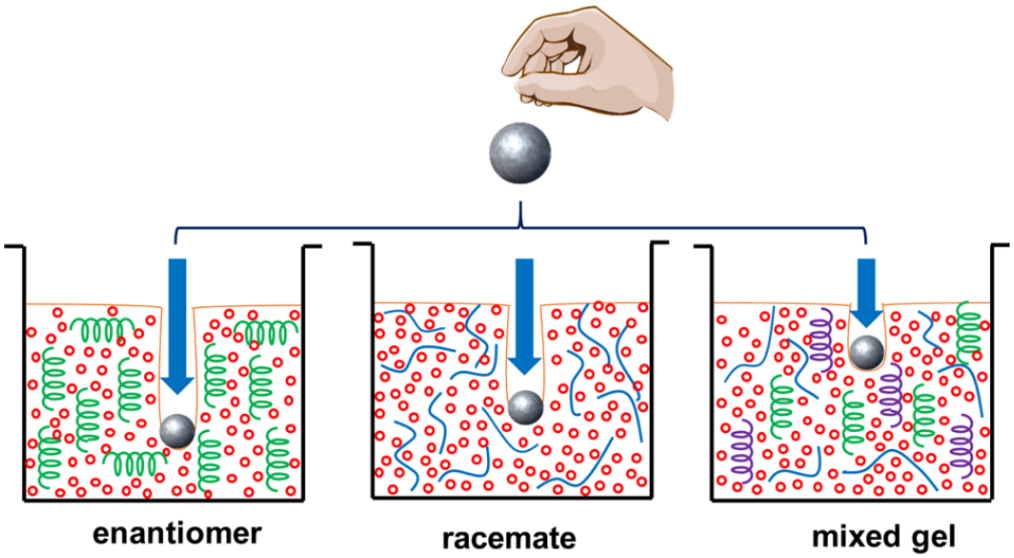

Figure 9. Enantiopure and racemic bis(urea) compounds, tagged with phenylalanine methyl ester, formed gels in multiple solvents. The racemate (1-rac) yielded a more robust gel structure compared to the enantiomers. The gel (1R+1S), formed by combining equimolar quantities of enantiomers (1R and 1S), exhibited enhanced thermal and mechanical stability compared to the individual enantiomers and racemate gels.[28] Reprinted with permission from ref. 28., Copyright 2018 American Chemical Society.

In the design of mixed gel systems, chirality can clearly play a key role. However, assembly can be directed by self-recognition through designing gelators with similar structural motifs instead of the same chirality.[25]

Afrasiabi and Kraatz'[29] research shows the importance of self-recognition when designing multicomponent gels. In the study, discrimination of compatible and non-compatible components guides the efficient assembly of the building blocks. A series of different Boc-L-

Phe-L-Lys(Z)-OMe (Z=carboxybenzyl) analogues were prepared, incorporating ferrocene or pyrene groups at the N-terminus. These groups were incorporated with the aim of creating a stimuli responsiveness for the hydrogel systems. Several mixtures exhibited gelation on various organic solvents under sonication (heating-sonication) and thermal (heating-cooling) conditions. The sequence of amino acids in the peptide-based gelator could be adjusted to promote the formation of either self-sorted or co-assembled structures. When amino acid sequences diverged, self-sorting occurred between gelators in a mixed system. Conversely, when the amino acid sequence was identical in opposite gelators, co-assembly occurred.[25]

5.2 Other design rules

The molecular structure of gelators alone does not determine how self-assembly occurs, as self-assembly is influenced by many other factors as well. Adams *et al.*[30] compared the two-component gels of gelators **9**-**11** (**9**+**10** and **9**+**11**) under the same conditions (Figure 10). Based on the molecular structures, the initial assumption could be that the mixed gels would behave similarly, but in fact, they work opposite to each other. The C-terminal amino acids in gelators **9** and **10** are different; therefore, the pKa values differ. If gelators **9** and **10** are dissolved at a higher pH, after which glucono-δ-lactone (GdL) is added to acidify the solution slowly (hydrolyzes creating an acidic environment), self-sorted nanofibers are observed. Although gelators **9** and **11** have the same substituent at the C-terminal amino acid, their gel is co-assembly by both gelators. According to the authors, the variance arises from the co-assembled micelles formed from **9** and **11** already at higher pH. Monitoring the pH revealed a plateau at pH 5.5. This pH value is between the individual pKa values of **9** (5.9) and **11** (5.3). This discovery supports the authors' theory that the co-assembled structures form first, and they transform into the final co-assembled gel as the pH value decreases. However, the precise mechanism behind this remains incompletely understood.[9]

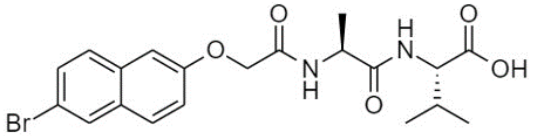

9

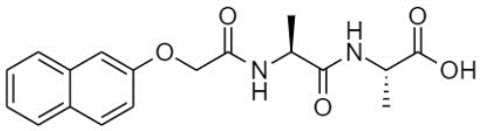

10

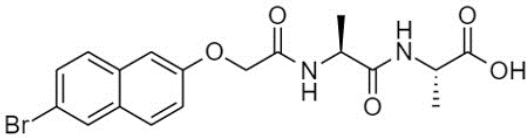

11

Figure 10. Structures of the dipeptides **9**, **10** and **11** used in the study.

5.2.1 Halogen substitution to a benzyl group

In addition to self-recognition motifs, methods based on other design principles have also been developed for designing multicomponent systems. Inspired by amyloid architectures, Nilsson *et al*.[31] investigated the impact of incorporating halogen substituents into the benzyl group of a single gelator in their mixed gels.[25]

The π-π stacking interactions within assembled gelator molecules can be influenced by the incorporation of a halogen substituent and the mechanical characteristics of the resulting gel can be impacted by the selection and placement of the halogen substituent. Offset π-π interactions between the non-substituted benzyl of the one gelator and the halogenated substituents on the benzyl ring of other gelator favored co-assembly. Complementary quadrupoles were not necessary for co-assembly. The design rules were elucidated through a system involving the co-assembly of an Fmoc-Phe with Fmoc-Phe gelator derivative containing a perfluorinated ring (Figure 11A). The perfluorinated gelator was able to assemble and gel independently when a solvent-mediated trigger was used (Figure 11B). Under the same

conditions, Fmoc-Phe formed a precipitate. However, when the two components were combined in a 1:1 ratio, gel formed without any signs of precipitation, indicating the incorporation of Fmoc-Phe into the fibers and co-assembly (Figure 11C).[25]

Replacing Fmoc-Phe with Fmoc-D-Phe in the mixed system prevented gel formation, signifying the complementary and selective nature of the interactions dictating co-assembly. Furthermore, the replacement of Fmoc-Phe with Fmoc-Leu also prevented gelation despite similar hydrophobicity between these gelators. This suggests that assembly cannot be driven by hydrophobic interactions alone.[25] The ability to control the temporal aspects of hydrogel assembly kinetics and mechanical characteristics by manipulating the identity and location of halogen substituents offers a valuable tool for advancing the development of these materials.[31]

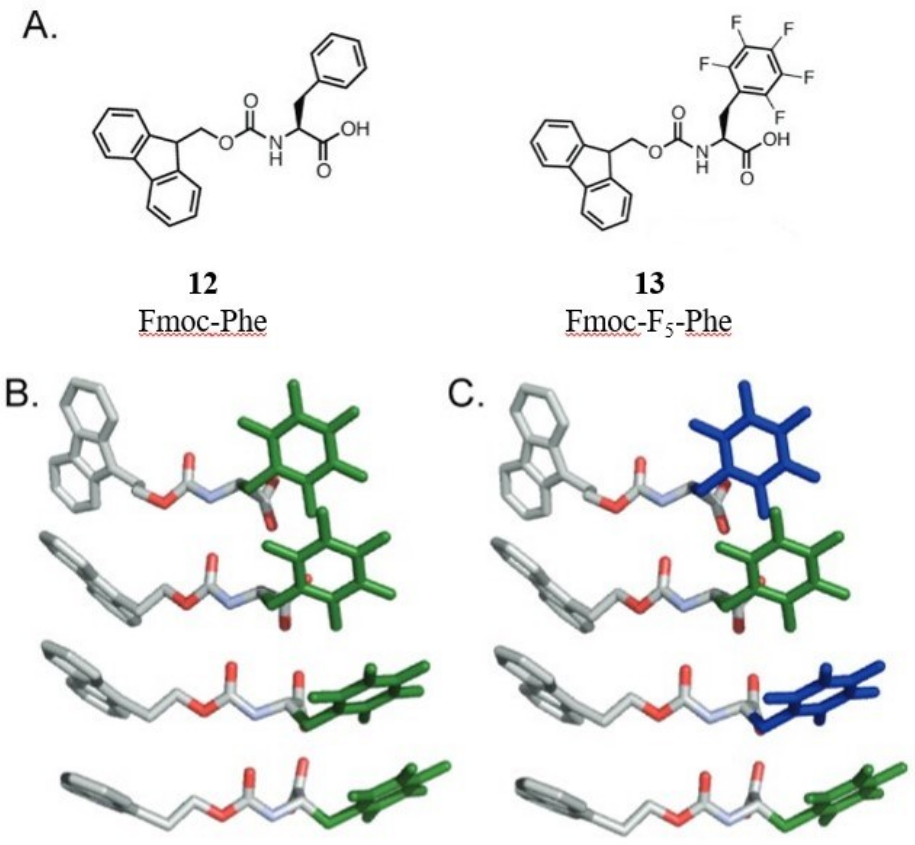

Figure 11. A) Chemical structures of Fmoc-Phe (**12**) and Fmoc-F_5-Phe (**13**). B) Suggested packing model for the self-assembly of Fmoc-F_5-Phe. C) Suggested arrangement for the packing of Fmoc-Phe (blue) and Fmoc-F_5-Phe (green) in co-assembled fibrils. Reprinted and adapted with permission from ref. 31., Copyright 2011 American Chemical Society.

5.2.2 Hydrophobicity and pH

Adams *et al.*[3] have studied the interactions of a dipeptide gelator (**13**) with non-gelling amphiphiles (compounds **14**-**18**). The study showed that under low pH, compound **13** can form gels with compounds **14**-**18**, and that the hydrophobicity of the non-gelling component notably impact the properties of the multicomponent systems (Figure 12). In the direct preparation of gels, Fmoc amphiphiles with a short alkyl chain (compounds **14**-**16**) and relatively high hydrophilicity have a minimal effect on gelator self-sorting. However, it was observed that when non-gelling amphiphiles have higher hydrophobicity (**17** and **18**), the components form a gel through co-assembly. The assembly pattern changes when gelation is initiated by the pH switching method. In this scenario, the gelator molecules co-assemble with the non-gelling component with a short hydrophobic linker. Therefore, utilizing a pH-switching method or increasing the hydrophobicity of the non-gelling component offers the ability to control the network type (co-assembly or self-sorting) of the multicomponent hydrogel. The properties of supramolecular gels depend on the chosen preparation method.[3]

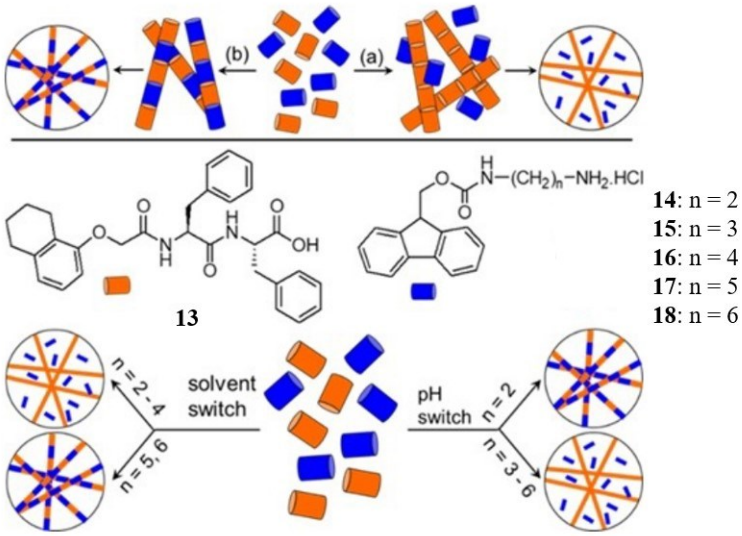

Figure 12. Top: Schematic presentation showing how the multicomponent gel from a gelator (orange) and a non-gelling compound (blue) can form through (a) self-sorting and (b) co-assembly. Bottom: Chemical structures of the gelator (**13**) and the non-gelling compounds (**14**-**18**). The assembly patterns are determined by the hydrophobicity of the non-gelling Fmoc-salts, with the outcome varying based on the chosen preparative pathway.[3]

Adams and his coworkers[32] prepared self-sorted hydrogel through sequential assembly, utilizing the natural pKa differences of the gelators (Figure *13*). The alanine-terminated perylenebisamide (PBI) **19** has two pKa values, 6.6 and 5.4, and the phenylalanine-terminated stilbene **20** has a pKa value 5.8. The gelators are initially dissolved at a higher pH, after which GdL is added to acidify the environment through the hydrolysis of GdL. With the gradual decrease in pH, it is expected that the gelator with a higher pKa will undergo self-assembly and form a gel first. However, at the first pKa of **19** (6.6), the gelator undergoes spontaneous aggregation into worm-like micelles, and gelation occurs only when the second pKa (5.4) is reached. Therefore, the fibers of stilbene-based **20** form first, and only after that the fibers of the PBI-based **19** form as the pH continues to decrease. [9,32]

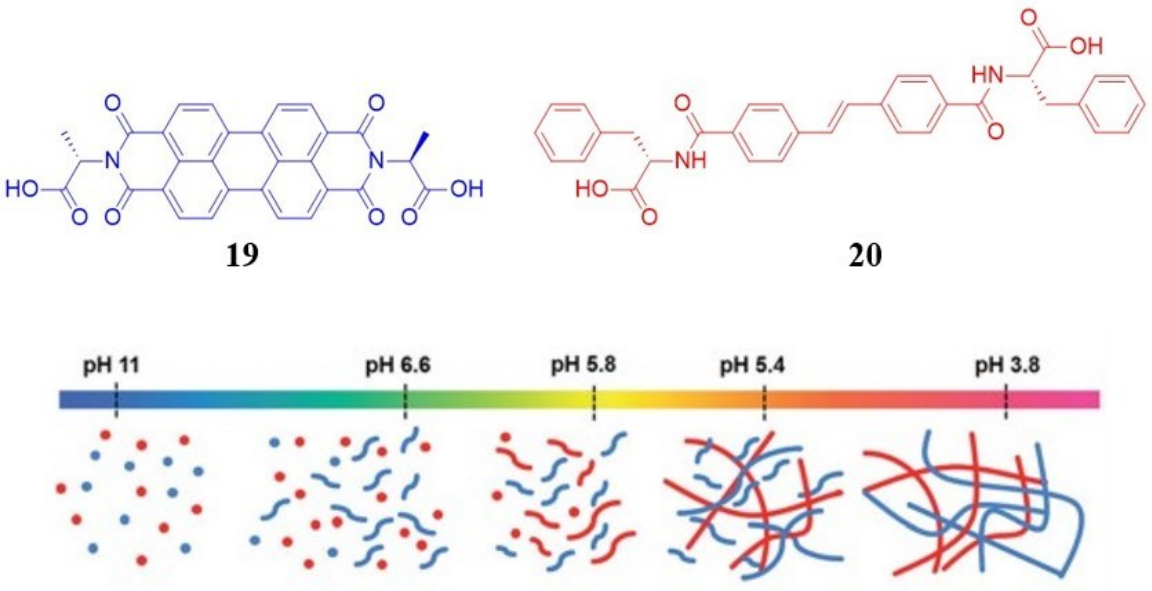

Figure 13. a) Molecular structures of the alanine-terminated perylenebisamide (PBI; **19**) and phenylalanine-terminated stilbene (**20**). b) Schematic representation of the stepwise self-assembly of gelators upon pH decrease. Flexible short structures describe the formation of worm-like micelles, whereas the longer and straighter structures represent the formation of fibers.[32] Reproduced and adapted from ref. 32., Copyright 2016 with permission from the Royal Society of Chemistry.

5.2.3 Kinetics

The resulting morphologies can be significantly influenced by the kinetics of the self-assembly process. Tovar *et al.*[33] prepared three separate π-electron units (oligo(p-phenylenevinylene), quaterthiophene and naphthalene diimide) within peptidic structures. They investigated self-sorting and random co-assembly of two-component photoconductive gels, composed of the same components, with the assembly being strongly influenced by the rate of acidification.[33]

To create a distinction in the pKa values of each component, Asp-Val-Val and Lys-Ala-Ala peptide sequences were selected for the oligo(p-phenylenevinylene)- and quaterthiophene-appended (OPV3; **21** and OT4-NDI; **22**) peptides, respectively (Figure 14). When the 1,4-distyrylbenzene, an oligo(p-phenylenevinylene), is photoexcited, it can transfer energy to an acceptor unit, quaterthiophene. In a similar manner, in its excited state, quaterthiophene transfer electrons to the naphthalene diimide in OT4-NDI. A control molecule, OT4-Ac (**23**), was also synthesized. In this molecule, the side-chain amines were acylated instead of using naphthalene diimide groups. With the help of the control molecule, it was possible to observe photonic energy-transfer events without the associated electron transfer.[33]

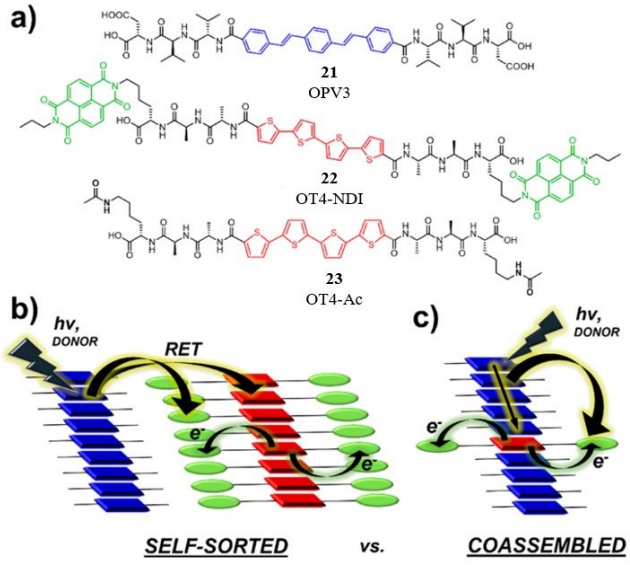

Figure 14. a) Molecular structures of the peptides OPV3 (**21**), OT4-NDI (**22**) and OT4-Ac (**23**), and b), c) illustration of potential energy dynamics, including resonance energy transfer (RET) and electron transfer events within the two-component peptide nanostructure with three π-electron units b) for the self-sorted and c) randomly assembled systems.[33] Reprinted and adapted with permission from ref. 33., Copyright 2017 American Chemical Society.

Both components, OPV3 and OT4-NDI, were dissolved at higher pH. The pKa value for OPV3 is 6.2, and for OT4-NDI, it is 6.5. When the pH of the system slowly decreases with the addition of glucono-δ-lacton (GdL), the the gelators have the opportunity to react to the pH change due to the slow kinetics. This difference in pKa values causes the gelators to start self-assembling at different pH levels, leading to the formation of self-sorted gels. If a rapid addition of HCl is used to trigger the assembly, the gelator molecules do not have time to react to the gradual change in pKa and co-assembled supramolecular polymers are formed. Self-supporting hydrogels were formed through both methods.[33]

These observations on the photophysical behavior of multichromophoric peptide assemblies are valuable. Self-sorting of the components is useful in forming p-n heterojunctions, while co-assembly is beneficial in creating photosynthetic mimics requiring high energy transfer efficiency.[33]

The stepwise control of multicomponent gels promotes the development of more intricate LMWG systems. Additionally, advances in the characterization methods of multicomponent systems allow real-time monitoring of nanofiber growth, thus helping to understand the mechanisms of gel formation mechanisms.[9]

6 Characterization of multicomponent gels

In addition to the primary assembly, the properties of the gels are also affected by how the fibers entangle, crosslink and interact. Therefore, it is important to understand the structure on a wider scale in addition to the primary assembled structures. For example, if we consider that self-sorted fibers are formed and one network is formed before the other, the properties of the gel are due to two networks. The properties depend on how these networks interact with each other or if they interact at all. For example, the formation of the first network can be influenced by the presence of the second (at that point un-gelled) component, and the presence of the first network can impact the formation of the second network. It has been shown that the presence of a non-gelling additive can remarkably affect the growing gel networks.[2]

Understanding the self-assembly of the system across various scales, from the molecular level to the multi-micron length scale, is important. The interactions at the molecular level determine the assembly in the primary structures. Different interactions between the formed primary fibers are observed on a nanometer scale. The spatial distribution of fibers might exhibit homogeneity or heterogeneity on the multi-micron length scale with possibly distinct underlying microstructures.[7,8]

The dynamic nature of the noncovalent interactions between the gelator molecules forming the supramolecular gel complicates the characterization of supramolecular gels.[34] To comprehensively investigate these soft materials and obtain information across these different dimensions, various techniques must be used (Figure 15).[2] Understanding the selection and combination of different characterization methods, aligned with the gelation mechanism, holds significant importance.[34]

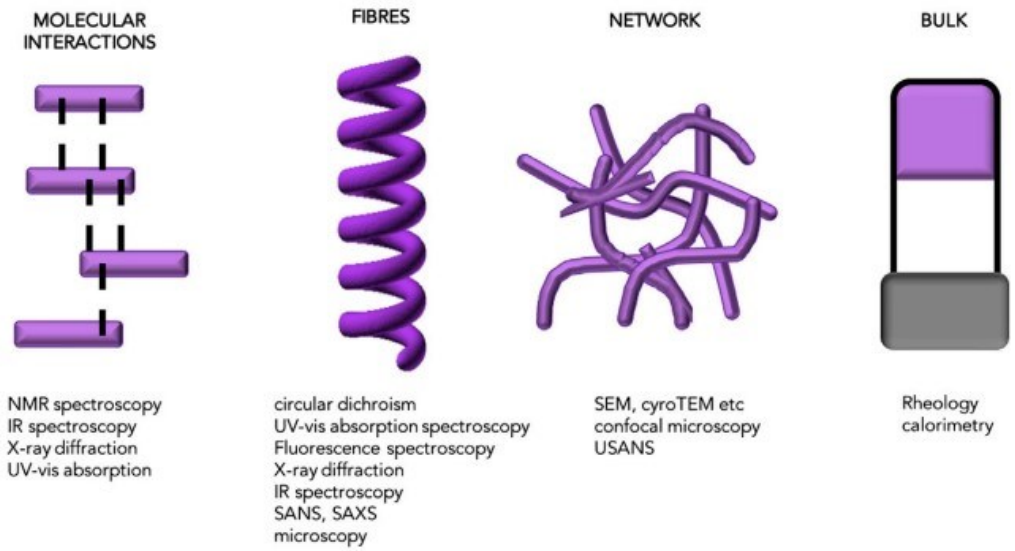

Figure 15. Different techniques are suitable for studying gel structure at a specific length scale.[15] Reprinted with permission from ref. 14., Copyright 2017 Elsevier.

6.1 Molecular level assembly

When gelators are mixed, their assembly can take place via self-sorting or co-assembly. At this scale, several analytical techniques such as UV-visible (UV-vis) absorption spectroscopy, infrared (IR) spectroscopy, fluorescence spectroscopy, and circular dichroism (CD) spectroscopy can be useful tools for investigating hydrogen bonding, molecular packing etc. The methods are based on dissimilarities either between individual components or the resulting network compared to the two original materials.[2]

6.1.1 Spectroscopy

UV-visible (UV-vis) absorption spectroscopy serves as a valuable tool for analyzing the aggregation states of molecules. It is commonly employed to determine whether aggregates exhibit H-aggregation or J-aggregation, forming extended stacks, etc. The co-assembly or self-sorting of a multicomponent system can also be investigated using these spectra. If some co-assembly were to occur, it is anticipated that the absorption of the two molecules would change due to alterations in the energy levels caused by aggregation On the other hand, in the case of self-sorting (or at least most self-sorting), no alteration in the absorption of the individual components is assumed, and the combined spectrum should resemble an overlay of the spectra for the two separate components. However, it can be challenging to determine whether these systems are randomly assembled, socially self-sorted or somewhere in between using this technique.[2]

Fourier-Transform Infrared (FT-IR) spectroscopy operates similarly to the Uv-vis spectroscopy. The overlap of two separate components may indicate self-sorting, while the difference in the spectrum for the mixed system compared to the spectra of the components suggests co-assembly. Additionally, FTIR can provide valuable information about how interactions occur, for example, between H-bonding or COOH groups. This technique offers information about the stacking of the molecules and can even be used to estimate how much co-assembly occurs.[2]

Fluorescence spectroscopy, a form of electromagnetic spectroscopy, is used to examine the fluorescence emitted by a sample. This technique has multiple applications in chemical, biochemical and medical research for analysing organic compounds.[34] In the study of multicomponent gels, fluorescence spectroscopy can be used to probe the molecular packing.[2] For example, Ulijn *et al.*[35] used fluorescence spectroscopy to study Fmoc-Gly-Gly, Fmoc-Phe-Phe, and a gel formed from their mixture. A 50:50 mixture of the Fmoc-Gly-Gly and Fmoc-Phe-Phe appeared to yield a more stable gel than single-component gels. Fluorescence spectroscopy measurements revealed increased interactions between molecules within the mixed gel. Fmoc-Phe-Phe and mixed gel exhibited an emission peak at 332 nm, in contrast to non-gelling peptide 1, which had an emission maximum at a wavelength of 320 nm (Figure *16*). This shift indicates the antiparallel overlap of fluorenes. Furthermore, a broad phosphorescence peak, primarily observed in the mixed gel, implies the stacking of multiple fluorenyl moieties. Studies have reported a reduction in the intensity of emission peaks, and a continuous redshift of these peaks during the formation of molecular hydrogels. This phenomenon is attributed to the formation of increasingly rigid networks within the gels.[36]

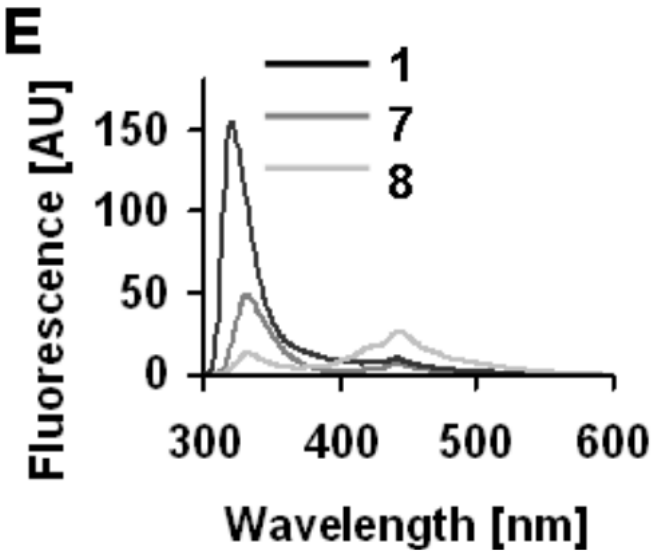

Figure 16. Fluorescence spectra of hydrogels from Fmoc-Gly-Gly, Fmoc-Phe-Phe and a 50:50 mixture of these peptides.[35] Reprinted with permission from ref. 35., Copyright 2006 John Wiley & Sons, Inc.

Circular dichroism (CD) relies on the differential absorption of right and left circularly polarized light. It is a convenient technique for investigating the inter- and intramolecular interactions and stereostructures of diverse categories of chiral supramolecules. The advantages of CD spectroscopy are its sensitivity, indestructibility, and rapidity. It typically requires only submicrogram-scale sample quantities to obtain valuable information about the intra- and intermolecular interactions within self-assembled systems, polymers, host-guest systems, and more. The sensitivity of CD spevtroscopy to molecular configuration and conformation makes it a more versatile tool for analyzing the structure of several chiral supramolecular systems compared to its parent achiral absorption spectroscopies such as IR and UV-vis spectroscopy.[34] In co-assembly cases, the CD spectrum differs from the expected sum of the component spectra. However, in self-sorted systems, it has been proven that the CD spectrum is a direct overlap of the sum of individual components' spectra. [2]

6.2 Fibre level assembly

Microscopy and small-angle scattering are the most commonly used techniques to study self-assembly at the fiber level. Also, computational methods have been employed to study the molecular packing of co-assembled or self-assembled materials. In the case of multicomponent gels, computational methods can be challenging. As the number of molecules involved in the calculations increases, the calculations become longer and more complex. The method also cannot take into account the changing conditions that occur when molecules self-assemble or the solvent environment. At the moment, most computational methods are based on information already collected from the sample, so it is more of a post-rationalization of results rather than a prediction of whether the sample is co-assembled or self-sorted.[2]

6.2.1 Microscopy

Optical microscopy lacks the necessary resolution for imaging the network formed by most LMWGs. Instead, scanning electron microscopy (SEM) or transmission electron microscopy (TEM) are commonly employed to study fiber structures.[2]

SEM, a type of electron microscopy, captures sample images through scanning the sample with a focused electron beam. These electrons interact with the electrons within the specimen, resulting in the generation of various signals. These signals can be detected and contain details about the composition of the sample and surface topography. Typically, the electron beam follows a raster scan pattern, and its position is correlated with the detected signal to create an image. SEM is a useful technique for studying the microscopic structure of self-assembled systems due to its large depth of focus and high lateral resolution.[34]

TEM, another a microscopy technique, operates by having an electron beam interact with the sample as it passes through it. The image is generated through the interaction between electrons and the sample. The image is then magnified and directed to an imaging device (sensor (CCD camera), layer of photographic film, or fluorescent screen). Providing the necessary resolution for detecting molecules at the subnanometer scale, TEM can observe the superstructures of the gelators self-assembled through multiple interactions. Consequently, making it a valuable tool for characterizing the structure of supramolecular gels. Important information about the gelation mechanism and process can be obtained by analyzing the shape and size of the aggregates.[34]

A broad spectrum of structures formed by LMWGs has been imaged, including fibers, tubes, helical structures, sheets, and hierarchical structures where primary structures can combine to form larger assemblies. One challenge in multicomponent systems is that distinguishing between gelators can be difficult, as many LMWGs often exhibit fiber structures with similar dimensions. Therefore, determining whether the structures consist of mixtures of fibers from the individual components or if new structures are formed can be extremely challenging.[2]

Moffat and Smith[37] examined mixtures of gelators **24**-**26** (Figure 17) with a bola-amphiphile-like structure (comprising a lysine head-unit attached to either end of a diamino dodecane spacer) to evaluate self-sorting during assembly. Equimolar mixtures of **24**+**25** and **25**+**26** were investigated using Field Emission Gun-SEM (FEG-SEM) imaging.

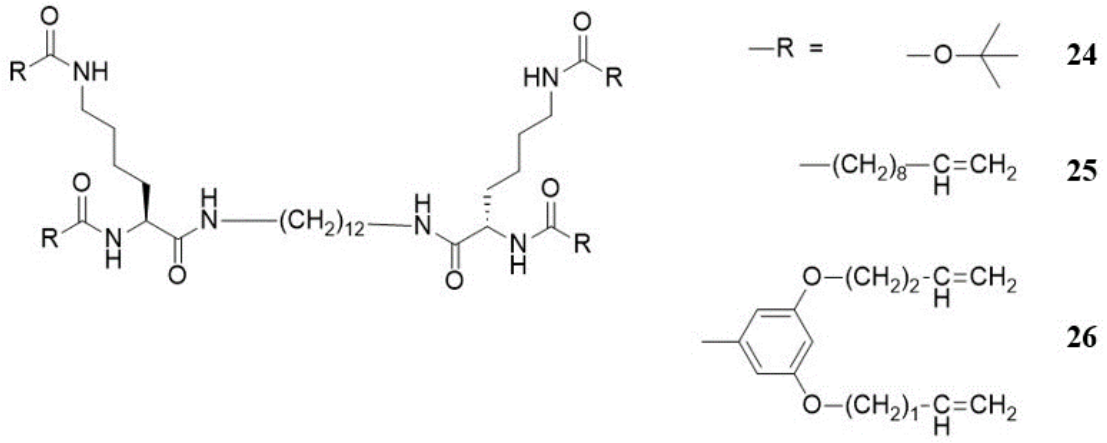

Figure 17. Structures of gelators **24**-**26**.

From the SEM images of the mixture of gelators **24**+**25**, it can clearly be stated that both gelators can self-sort into distinct individual fibers. In the image (Figure 18), two fiber types with significantly different diameters can be observed. The dimensions of these two fiber types were the same as those of the gelators when they were examined separately. The diameters of the larger fibers vary from 50 to 125 nm, and the diameters of the smaller fibers are approximately 25 nm. The clustering of similar fibers can also be seen in FEG-SEM images. It is uncertain whether aggregation of similar fibers occurs during the drying of the sample or whether some degree of nanoscale fiber sorting occurs in the solvated gel as a result of fiber-fiber interactions.[37]

For the mixture **25**+**26**, FEG-SEM images revealed an inability to self-sort. The mixture of gelators **25**+**26** formed a gel, and approximate fibers were observed in the images (Figure 18). The diameters of the fibers detected in the mixture were about 90 nm larger than the diameter of either gelator separately. A granular structure was also observed in these fibers. This may be due to the clustering of vesicles within these fibers. Regardless, it is evident that the nanoscale morphologies of gels **25** and **26** change significantly during mixing, unlike gelators **24** and **25**.[37]

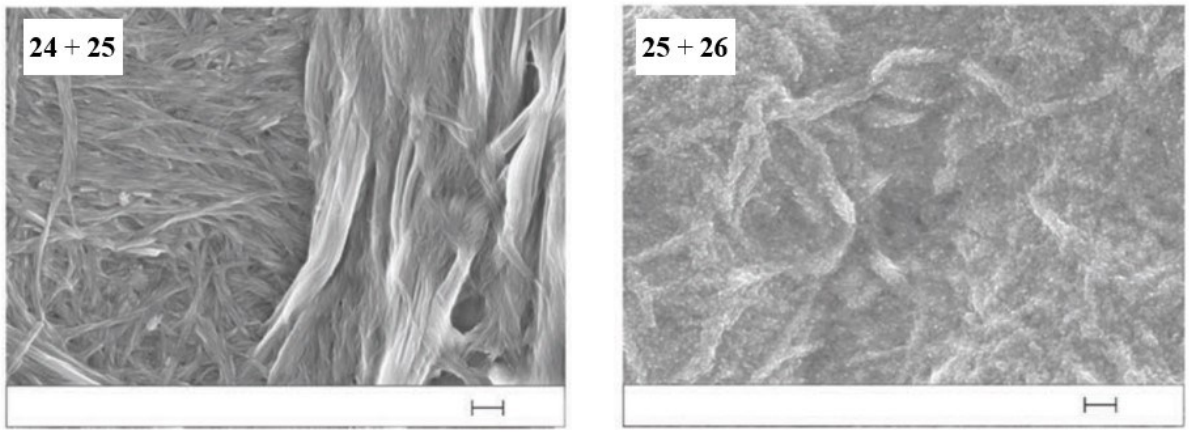

Figure 18. FEG-SEM images of mixtures **24**+**25** and **25**+**26**.[37] Used and adapted with permission of RSC, from Controlled self-sorting in the assembly of 'multi-gelator' gels, Moffat, J. R. and Smith, D. K., 2009; permission conveyed through Copyright Clearance Center, Inc.

6.2.2 Small angle scattering

When examining "soft" biological materials using microscopy, the problem is that the sample requires processing such as dilution, drying and freezing.[38] In addition, it is common in SEM to inject metal into the structures of the samples and in TEM to stain the structures with, for example, a heavy metal salt. All this processing can cause artefacts in the morphology of the sample.[39] Small angle scattering (SAS) enables the characterization of bulk samples of such "soft" materials in their wet state without any processing and can, therefore, be a very useful tool alongside microscopy (Figure 19).[38]

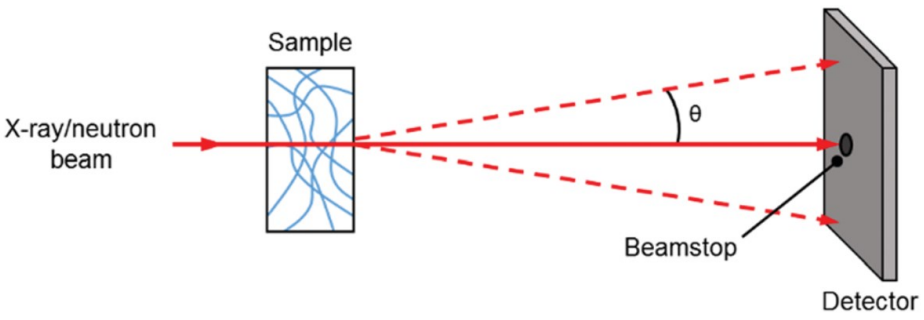

Figure 19. Schematic illustration of a small angle scattering (SAS) analysis.[40] Reproduced from Ref. 40., Copyright 2022 with permission from the Royal Society of Chemistry.

SAS allows the investigation of objects and features on the scale of 10-500 nm, making it particularly suitable for studying the self-assembly of proteins and peptides.[38] To examine primary fiber structures, small angle X-ray scattering (SAXS) and small angle neutron scattering (SANS) can be used and for investigating longer length scales and thus the network elements, ultra small angle neutron scattering (USANS) can be employed. Typically, scattering data is fitted to a model. For LMWGs, the most suitable fits are usually a cylinder, a flexible cylinder, or some other long anisotropic structure. Fitting provides information on parameters like the length, the radius of the structure, and more. One drawback is that often access to large-scale facilities is required. Moreover, SANS also demands contrast, typically achieved by employing deuterated LMWG or deuterated solvent. This results in a system that is not identical to those used in other techniques, and it also increases costs.[2]

These scattering techniques can be employed when examining multicomponent gels to determine whether co-assembly or self-sorting has occurred. This requires that the resulting new network exhibits significant distinction from the two individual components, or the two networks scatter notably differently.[2]

MacLachlan[41] and his research group investigated various multicomponent gels formed by three amino acid-based LMWGs (Figure 20) and compared their properties to the single-component gels of these gelators. They used SAXS to study the self-assembly of the gels.

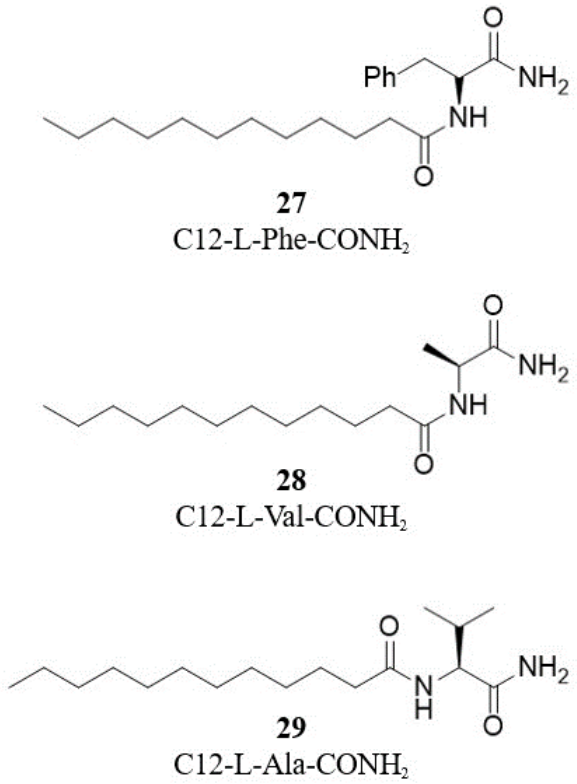

Figure 20. Molecular structures of the amino acid based gelators **27**, **28** and **29** used in the study.

Figure 23 shows the azimuthally averaged SAXS data of components **28** and **29** and mixture **28+29** (total concentration of all gels is 20 mg/mL in decane, with the mixture in equimass ratio). An expanded peak is observed for the mixture of **28+29**, shifted from the individual components due to distinct structural assembly. In the case of self-sorting, one would anticipate the peaks occurring at the same q-values and the mixture to exhibit the characteristics of both individual compounds. However, in this case, the mixtures exhibit peaks and fiber morphologies that are absent in the individual components, signifying the co-assembly taking place in the mixed system.[41]

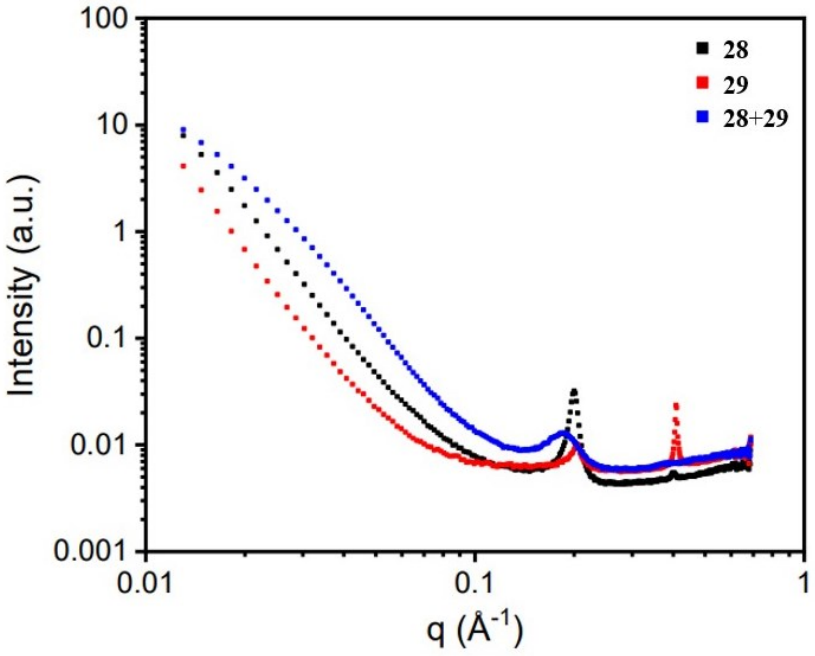

Figure 21. SAXS data for individual compounds **28** and **29** and mixture **28+29**.[41] Reprinted and adapted with permission from ref. 41., Copyright 2021 American Chemical Society

Sometimes microscopy data and scattering data provide discrepant information about the structure. Because scattering data is collected in a wet state, it is reasonable to assume that sample drying in microscopy has caused artefacts, especially if the dried structures have a larger apparent radius than indicated by the scattering data.[39] This was also observed by MacLachlan *et al.*[41] in their study. Based on the SEM images, the average fiber width for the mixtures **27**+**28** and **27+29** was approximately 70 nm and for the mixture **28+29**, it was about 60 nm. When SAXS data were fitted to a flexible cylinder model, the radius of the fibers could be determined. The radii of the fibers in the multicomponent gels were determined to be 40 Å, 43 Å and 48 Å for mixtures **27+28**, **27+29** and **28+29**, respectively. These estimates for fiber diameters are significantly smaller than those obtained from SEM image analysis. This is due to drying artefacts and the sample preparation.[41]

6.3 Network-level assembly

In general, microscopy and scattering techniques provide information about the primary fibers. However, understanding the nature and relative extent of cross-linking and lateral associations of fibers is challenging. Consequently, the networks typically need to be distinguished through inferential means. At the network level, the analysis involves the examinations of physical properties, melting point, and rheology.[2]

6.3.1 Physical properties

Inferring the type of network based on visual observations or behavioral changes is possible. However, changes in properties may not necessarily explain the precise aggregated nature of the samples or the extent of assembly. Yet, it can serve as a quick indicator of the assembly type. For instance, indications of co-assembly can be obtained if two samples that independently form transparent, stable gels are mixed, and their mixture then yields a turbid gel. However, this visual transformation might also arise due to variations in concentration or ineffective mixing of the samples. Therefore, other techniques should be used.[2]

The kinetics of changes in turbidity during gelation can provide information about different processes occurring.[2] For example, Gazit *et al.*[42] prepared two-component hydrogel from Fmoc-modified tyrosine (Fmoc-Tyr; **30**) and Fmoc-3,4-dihydroxyphenylalanine (Fmoc-DOPA, **31**) (Figure 22) and observed alterations in turbidity over time for the combined and single gelators to gain information about the organization and assembly kinetics.

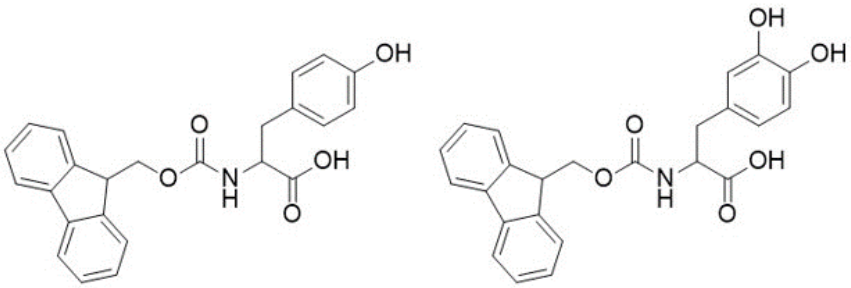

30
Fmoc-Tyr

31
Fmoc-DOPA

Figure 22. Chemical structures of Fmoc-Tyr (**30**) and Fmoc-DOPA (**31**).

The turbidity of Fmoc-DOPA hardly changed over 100 minutes, whereas the turbidity of Fmoc-Tyr gradually decreased significantly over 10 minutes. Interestingly, the turbidity of the two-component gel decreased gradually after a short delay, and its endpoint value was between that of the individual components (Figure 23).

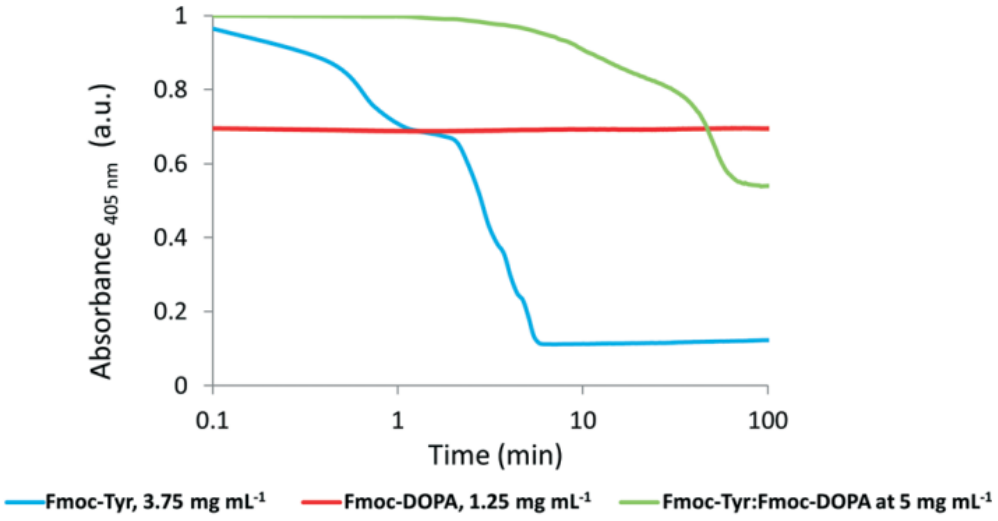

Figure 23. Graph illustrating the turbidity changes throughout gelation process of the single components Fmoc-Tyr (blue) and Fmoc-DOPA (red) and the two-component gel (green).[42]

In some cases, self-sorting can be observed by the eye, but this is extremely rare. For example, if a component shifts from a gel to crystal state within a single-component gel and this transition is also observed in a multicomponent gel, with a gel remaining intact, it indicates the formation of a self-sorted interpenetrating gel network. In a co-assembled system, the gel-to-crystal transition would likely to disrupt the entire gel network.[2]

6.3.2 Melting point

Measuring the gel's melting temperature (T_{gel}) is a conventional method in gel studies. This temperature is considered indicative of the network in the gel and is typically determined by the vial inversion method. Once the gel network reaches a molten state, the sample flows upon inverting the vial.[2]

The Moffat and Smith[37] mentioned earlier in section 6.2.1 also investigated the melting temperatures of gelator mixtures **24**+**25** and **25**+**26** (Figure 17). Figure *24* shows a graph depicting the thermal stability of gelators **24**, **25** and **26** and mixtures **24**+**25** and **25**+**26** as a function of gel concentration in styrene-divinylbenzene.

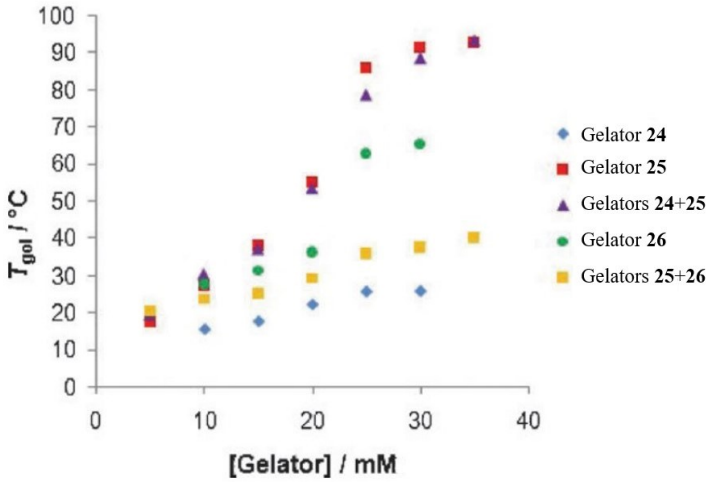

Figure 24. Graph illustrating the thermal stability as a function of gelator concentration on styrene-divinylbenzene (9:1).[37] Used and adapted with permission of RSC, from Controlled self-sorting in the assembly of 'multi-gelator' gels, Moffat, J. R. and Smith, D. K., 2009; permission conveyed through Copyright Clearance Center, Inc.

It can be seen from the graph that the thermal stability of mixture 1+2 is exactly the same as that of gelator 2 alone. The gel formed by gelator 1 is thermally less stable and does not seem to affect the ability of gelator 2 to form an efficient gel network. This suggests that the formed gel network is similar to that formed by a single gelator 2, i.e., self-sorting occurred. Based on thermal studies only, it cannot be concluded whether gelator 1 forms an independent gel network because it would 'melt' at a lower temperature than the macroscopically observed T_{gel} value. However, using FEG-SEM, it was confirmed that both gelators formed self-sorted fibers. Conversely, the thermal stability of the mixture 2+3 was significantly lower than that of either gelator alone. This indicates that these two gelators interfere with each other's self-assembling ability on a nanoscale. This is consistent with the fact that these two gelators have similar packing modes and thus exhibit co-assembly.[37]

6.3.3 Rheology

The mechanical properties of bulk gel sample samples are analyzed using rheology. Rheological properties are influenced by factors such as the morphology of the fibers, fiber concentration and strength, the spatial distribution of fibers and the type and quantity of cross-links. Since several variable factors influence rheological properties, identifying the exact reason why a particular gel is stiffer than another can be very challenging.[2]

In the case of multicomponent gels, it is difficult to choose which data should be compared. In most cases, the multicomponent gel is made by incorporating the concentrations of the single-component gel into the multicomponent system, and the rheological properties of individual single-component gels are then compared to those of the multicomponent gel. For example, if gelators 1 and 2 are at a concentration of 5 mg/mL in single-component gels, these concentrations are transferred to the multicomponent system, resulting in a total concentration of 10 mg/mL. The concentration typically affects the rheological properties of such gels, meaning that the number of fibers increases as the concentration of gel increases. Therefore, it would be highly likely that the storage modulus (G') and loss modulus (G'') values of the multicomponent gel would be higher. However, this is not always observed and rarely commented upon.[2]

Co-assembly and self-sorting of the system cannot, therefore, be determined based on the values of G' and G'' alone. There are examples of systems where the moduli of the system increase during mixing as compared to the single components.[2] For instance, Li *et al.*[36] reported a short peptide-based gelator system where a combination of two gelators resulted in a gel possessing a storage modulus at least ten times greater than that of each single-component gel. The gelators used in the study were phenothiazine-Gly-Phe-Phe-Tyr (PTZ-GFFY; **32**) and naphthalene-Gly-Phe-Phe-Tyr (Nap-GFFY; **33**) (Figure 25).

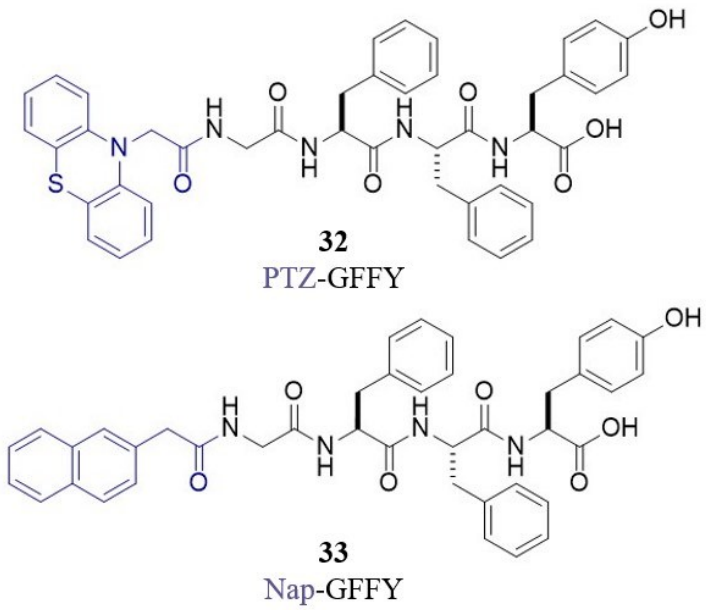

Figure 25. Molecular structures of phenothiazine-Gly-Phe-Phe-Tyr (PTZ-GFFY; **32**) and naphthalene-Gly-Phe-Phe-Tyr (Nap-GFFY; **33**).

Both gelators independently formed hydrogels using the heating-cooling method, but the mechanical characteristics of the gels were quite weak. The storage modulus (G') of PTZ-GFFY was only about 500 Pa, and that of Nap-GFFY was about 150 Pa (gelator concentration 1.0 wt%, frequency value 0.1 rad/s). The mixing of these gelators also resulted in the formation of a hydrogel (final concentration of 0.5 wt% for both) using the heating-cooling method. The storage modulus (G') of this two-component gel was about 5 000 Pa (frequency value 0.1 rad/s), i.e. at least ten times bigger than the G' value of each individual single-component gel (Figure 26).[36] Such enhancement in mechanical properties can result from several different

factors. Simply, it may be due to the system containing more gelators. On the other hand, it could also result from the formation of new fibers as a consequence of co-assembly, making the system stronger (e.g., by incorporating molecules that cross-link) compared to individual component systems. Alternatively, if self-sorting has occurred, the strength of the gel may have increased due to favourable interactions among the fibers, leading to entanglement and an increase in hydrogen bonding within the system.[2]

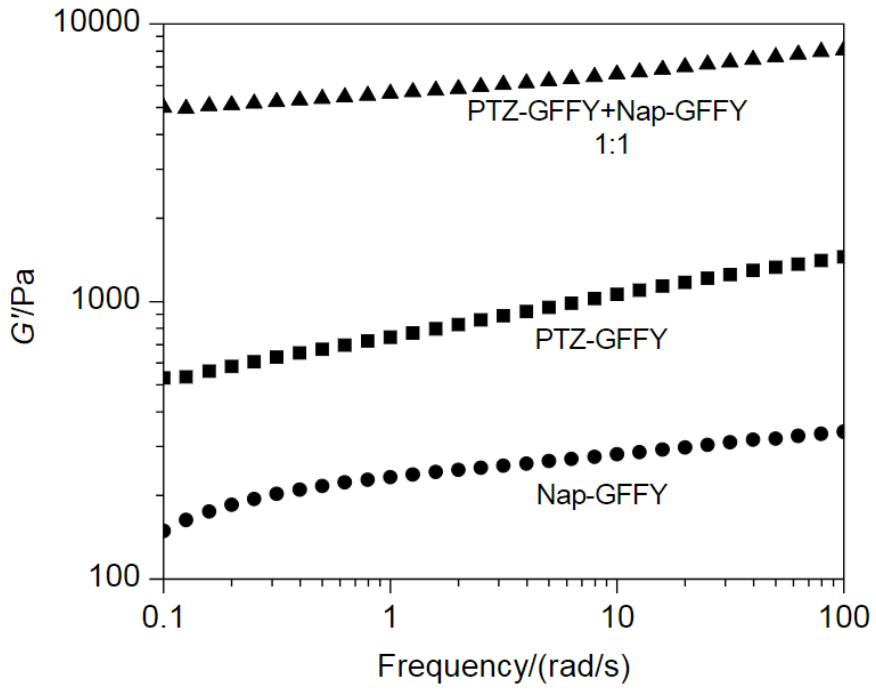

Figure 26. Rheological measurements in the dynamic frequency sweep mode for two-component gel PTZ-GFFY (0,5 wt%) + Nap-GFFY (0,5 wt%) and single-component gels of PTZ-GFFY (1 wt%) and Nap-GFFY (1 wt%).[36] Reprinted with permission from ref. 36., Copyright 2014 John Wiley & Sons, Inc.

7 Biomedical applications

In nature, the multicomponent self-assembly of various building blocks through noncovalent interactions generates numerous intricate and highly ordered architectures. Peptides and amino acids are utilized in creating supramolecular gels to construct and mimic these natural complexes. The extracellular matrix (ECM) is a commonly mimicked architecture with applications in tissue regeneration, drug delivery, and 3D cell culture. The peptide biomaterials used in these applications are usually single-component systems, thus limiting the level of functional and structural diversity and complexity. Furthermore, they struggle to replicate the complicated structure of natural ECM accurately because they only consist of peptide fibers. Multicomponent self-assembly provides diverse morphologies, molecular functional complexity, and tunable mechanical properties thus offering a better opportunity to produce materials that mimic natural ECM.[11]

7.1 Tuneable biomaterials

Kraatz *et al.*[11] created a multicomponent gel library aiemed at mimicking the complexity of the natural extracellular matrix (ECM). They investigated the addition of multiple biomolecules found within natural matrices (vitamins, carbohydrates, amino acids, building blocks of hyaluronic acid and combinations of these classes) to a myristyl-Phe-Phe-OH (C14-FF) hydrogel (Figure 27).

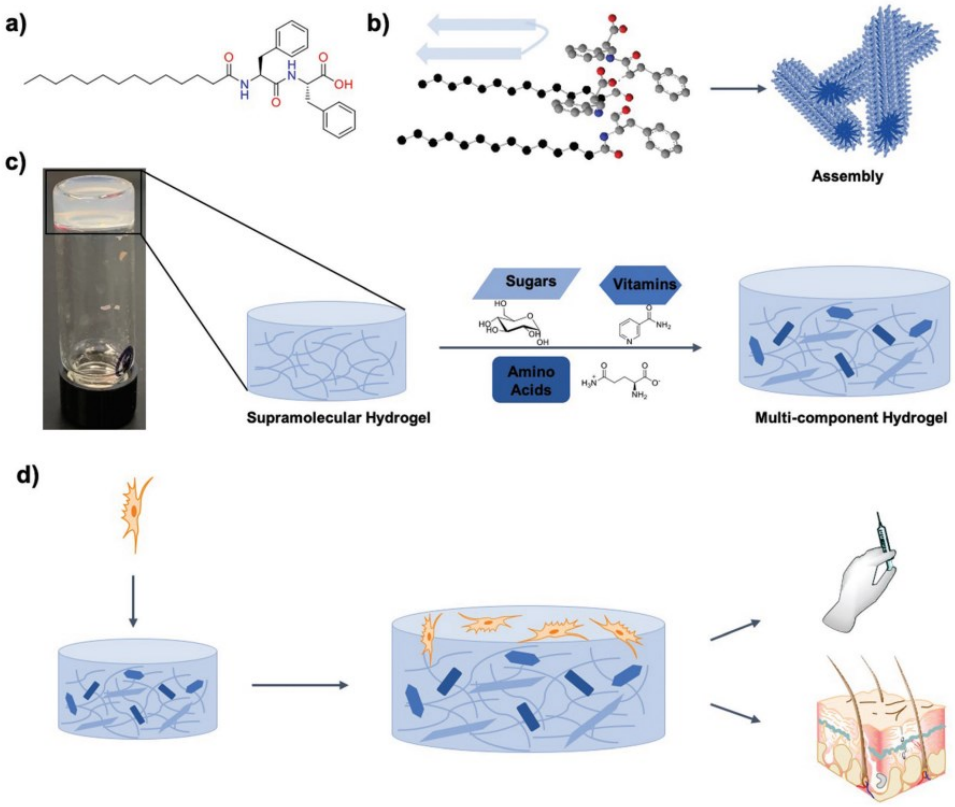

Figure 27. a) The chemical structure of the peptide amphiphile myristyol-Phe-Phe-OH (C14-FF), b) the assembly of individual C14-FF molecules into parallel β-sheets, forming long fibers, c) an inverted vial test of C14-FF hydrogel in PBS buffer after self-assembly, and illustration of the addition of diverse biological components, including sugars, amino acids, and vitamins, integrated into the gel matrix for the development of multicomponent hydrogels, d) exploration of cell viability in multicomponent hydrogels with potential applications in tissue engineering.[11] Used with permission of RSC, from Multi-component peptide hydrogels – a systematic study incorporating biomolecules for the exploration of diverse, tuneable biomaterials, Falcone, N.; Shao, T.; Andoy, N. M. O.; Rashid, R.; Sullan, R. M. A.; Sun, X., Kraatz, H.-B., 8, 2020; permission conveyed through Copyright Clearance Center, Inc.

The selection of components was guided by the composition of natural ECM. Carbohydrates participate in the structure of proteoglycans and as starch mimics. Glucuronic acid (GA) and N-acetyl glucosamine (NAG) form the main components of the matrix, hyaluronic acid. Collagen promotes structural integrity, whereas polylysine functions as a cell adhesion compound. The selection of mixtures was determined by incorporating biomolecules from various classes. The number of components gradually increased from mix 1 to 3. The ratio of

the C14-FF compound to the component was 80:20 (also 0.05% in PBS) and the overall concentration of the gels was 0.05% w/v (PBS, minimum gel concentration). The adaptability of the C14-FF compound to gel was evident, as all combinations of components successfully formed a hydrogel. All components used in the study and some essential properties (melting temperature of the gels (T_{gel}), the hydrogel stiffness (G'), and fibre widths ((nm) observed using AFM) are listed in Table 1.[11]

Table 1. A list of biological components examined with C14-FF hydrogel and their documented T_{gel} (°C), storage modulus (G' Pa^{-1}) and average fiber widths (nm) determined by AFM.[11]

Compound	**T_{gel} ± 4 (°C)**	**Storage modulus (G' Pa^{-1})**	**Fiber width (nm)**
C14-FF	48	264 ± 8	32 ± 7
C14-FF + polylysine	44	300 ± 80	110 ± 30
C14-FF + starch	50	210 ± 40	70 ± 20
C14-FF + N-acetyl glucosamine (NAG) + glucuronic acid (GA)	45	370 ± 20	50 ± 10
C14-FF + starch + polylysine (mix 1)	44	290 ± 30	110 ± 30
C14-FF + nicotinamide + biotin + riboflavin (vitamins)	46	180 ± 10	90 ± 20
C14-FF + glucose + polylysine + nicotinamide (mix 2)	43	220 ± 20	140 ± 40
C14-FF + glucose + glutamine + polylysine + biotin + riboflavin (mix 3)	41	200 ± 30	60 ± 11
C14-FF + collagen	50	410 ± 80	90 ± 20
C14-FF + glutamine	46	420 ± 30	70 ± 10
C14-FF + glucose	48	600 ± 50	70 ± 10

When comparing the G' values of the C14-FF + component hydrogels with single-component C14-FF hydrogel, it was observed that certain components (glucose, glutamine, collagen, NAG+GA, polylysine and mix 1) slightly enhanced the stiffness of the material, while others (mix 2, mix 3, vitamins and starch) reduced it, allowing the manipulation of mechanical properties through the addition of components. The mechanical rigidity of hydrogels has been showed to be a critical factor in the design of ECM mimics. For example, in bone regeneration applications, a 1 kPa hydrogel may not be suitable since the reported elasticity of bone cells is 730 kPa. On the other hand, collagen formulations with G' typically exceeding 100 Pa can be utilized for mammalian cells because the minimum requirement to sustain these cells in suspension is 50-100 Pa. By adjusting the concentration of the gelator and the amount of biocomponents, biomaterials can be designed to meet the specific needs of each organ, tissue or matrix.[11]

In addition to mechanical fine-tuning, these multicomponent hydrogels have many beneficial properties, such as diverse morphologies, cell compatibility, and self-healing. Overall, these multicomponent gels exhibit properties that potentially represent the natural ECM better than single-component gel systems. A library of such multicomponent gel systems can be used as a model to study functions and interactions in the ECM, as well as applications such as tissue regrowth and healing.[11]

7.1.1 Bone regeneration

Natural bone is an organic-inorganic nanocomposite with unique mechanical properties. However, bones can become diseased or damaged, requiring challenging orthopedic surgeries. The use of bone grafts (autografts, allografts, and xenografts) is associated with several limitations, including increased risk of infections, limited availability and cost of sample preparations, storage, and handling. To address these challenges, bone tissue engineering has emerged as a potential alternative treatment. The aim is to mimic its surrounding microenvironment and the natural state of bone tissue. This strategy is based on the *in vitro* creation of engineered graft materials intended for clinical use in *in vivo* bone defect reconstruction.[43]

Adler-Abramovich *et al.*[43] designed and synthesized peptide-based multicomponent hydrogels using two building blocks, Fmoc-FF (**34**) and Fmoc-Arginine (Fmoc-R, **35**). Arginine moiety mediates high affinity to hydroxyapatite (HAP), which was incorporated into the hydrogels to form three-dimensional scaffolds intended for bone tissue regeneration (Figure 28). HAP readily dissolves, creating a mildly alkaline environment and a high calcium ion layer. This

promotes osteoblast proliferation, adhesion, and matrix secretion, consequently enhancing the mechanical properties of the composite material.

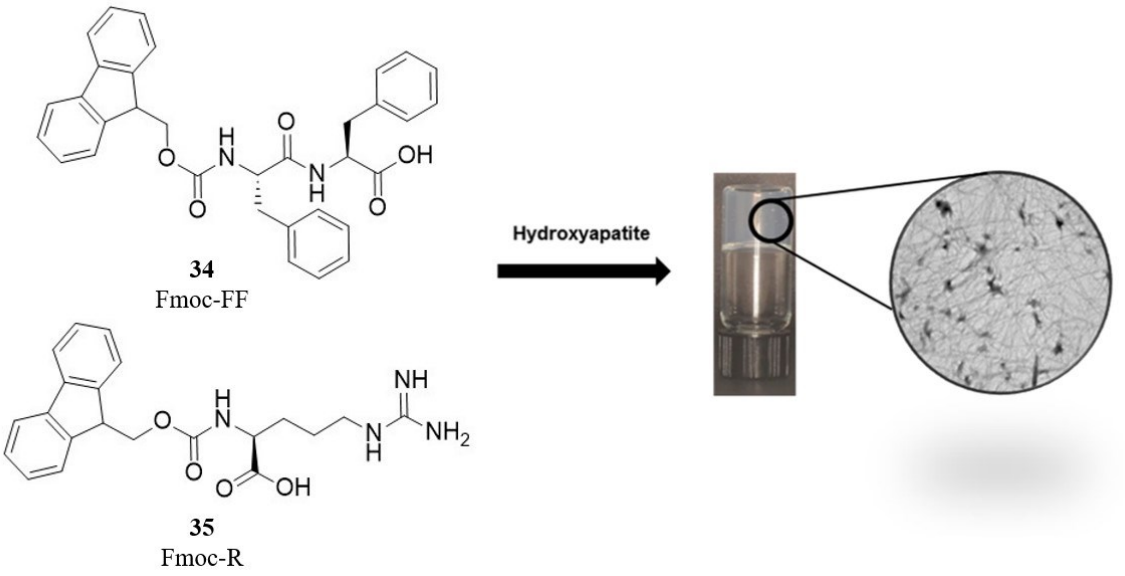

Figure 28. A multicomponent peptide-based hydrogel comprised fluorenyl-9-methoxycarbonyl-diphenylalanine (Fmoc-FF; **34**), influencing the rigidity and stability, and Fmoc-arginine (Fmoc-R; **35**), which contributed significant affinity for hydroxyapatite (HAP) due to the arginine moiety.[43] Reprinted and adapted with permission from ref. 43., Copyright 2017 American Chemical Society.

Fmoc-FF and Fmoc-R were combined in different ratios of 3:1, 1:1 and 1:3, both without HAP and including HAP. Fmoc-FF and Fmoc-R hydrogels alone were also prepared, with and without HAP. All hydrogels were prepared using a solvent switch method in DMSO/water medium (total DMSO concentration of 5 %). These hydrogels combined with HAP were composed of a nanoscale fibrillar network exhibiting a β-sheet secondary structure. Beyond serving as a crucial mineral in bone tissue regeneration, the study highlighted that the incorporation of HAP also enhances the mechanical stiffness of these hybrid hydrogels (Figure 29). For example, Fmoc-FF:Fmoc-R 3:1 HAP-hydrogel showed significant mechanical rigidity, reaching up to ~29 kPa. The hydrogels also maintained *in vitro* cell viability and facilitated cell adhesion. These organic-inorganic peptide-based hydrogels, composed of multiple components, exhibit potential to act as functional biomaterials for bone regeneration.

This potential arises from the incorporation of calcium bone particles, improved mechanical properties, and enhanced cell viability and adhesion.[43]

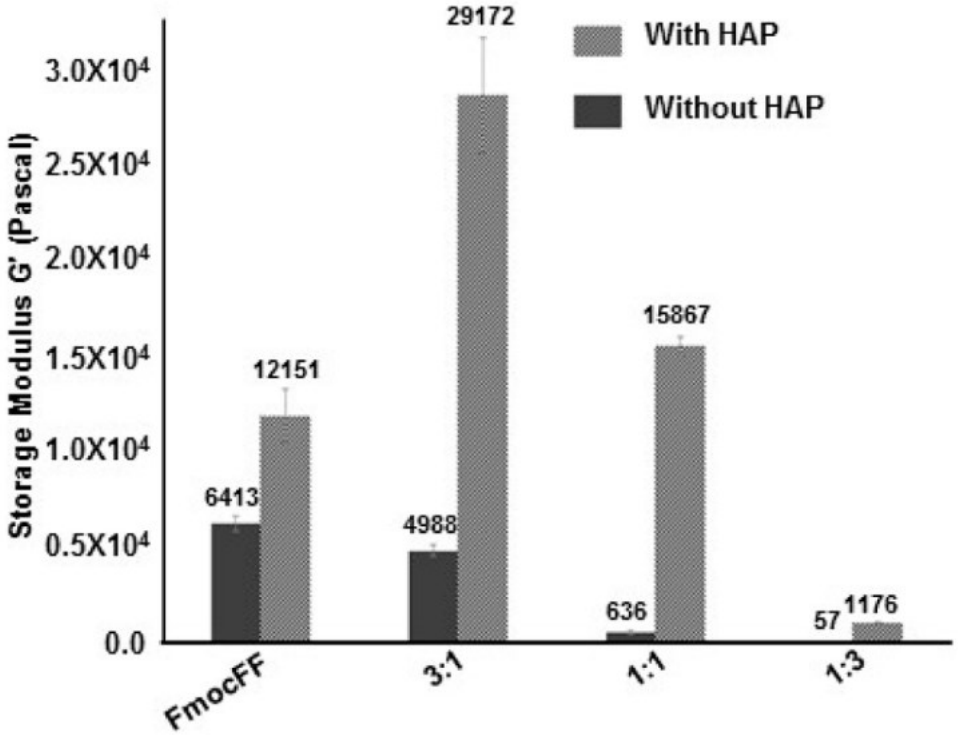

Figure 29. End point storage modulus (G') in time sweep rheology of the hydrogels: the value of mechanical storage modulus at 1 h for Fmoc-FF with and without HAP, Fmoc-FF:Fmoc-R 3:1 and 1:1 with and without HAP, 12 h for Fmoc-FF:Fmoc-R 1:3 without HAP, and 6 h for Fmoc-FF:Fmoc-R 1:3 with HAP.[43] Reprinted with permission from ref. 43., Copyright 2017 American Chemical Society.

7.2 Drug delivery

Hydrogels can be utilized diversely as drug delivery systems. They possess useful features such as bioadhesion, increased biological bioavailability, spatially and temporally controlled release, and protection against drug degradation. Thanks to their adjustable and programmable physicochemical properties, it is possible to load and encapsulate multiple active

pharmaceutical ingredients (APIs) into hydrogels, including antibodies, drugs, therapeutic agents, or signaling molecules. Drugs are typically entrapped within the hydrogel network, so the hydrogel mesh size can be a crucial factor in controlling the release profile. Other mechanisms, such as association with cyclodextrins, the formation of amide bonds and electrostatic interactions, are also possible. Extensive research has focused on exploring Fmoc-FF hydrogel as a promising drug delivery system. However, it has limited stability in a pH 7.4 phosphate-buffered saline (PBS) solution, which has complicated its *in vivo* applications. To address this challenge, numerous hybrid hydrogels based on Fmoc-FF have been proposed.[22]

In 2011, Qi *et al.*[44] reported a novel peptide-polysaccharide hybrid hydrogel designed serving as a promising carrier for the sustained delivery of hydrophobic drugs. This hybrid hydrogel was prepared from Fmoc-diphenylalanine and konjac glucomannan (KGM), through the molecular self-assembly of Fmoc-FF in a KGM solution. KGM is a natural water-soluble polysaccharide consisting of D-glucose and D-mannose.[45] Within this hybrid hydrogel, self-assembled peptide nanofibers intertwined with the KGM chains, resulting in a gel network that was highly hydrated and rigid. Findings from stability testing and rheological analysis revealed that the hybrid hydrogel exhibited significantly increased mechanical strength and stability in comparison to the Fmoc-FF hydrogel alone. In the study, docetaxel was used as a representative model for a hydrophobic drug. It was incorporated into hydrogel to examine *in vitro* release characteristics. The controlled and sustained release of drugs from this hybrid hydrogel depended on the KGM concentration, molecular weight, ageing time, and β-mannanase concentration (Figure 30).[44]

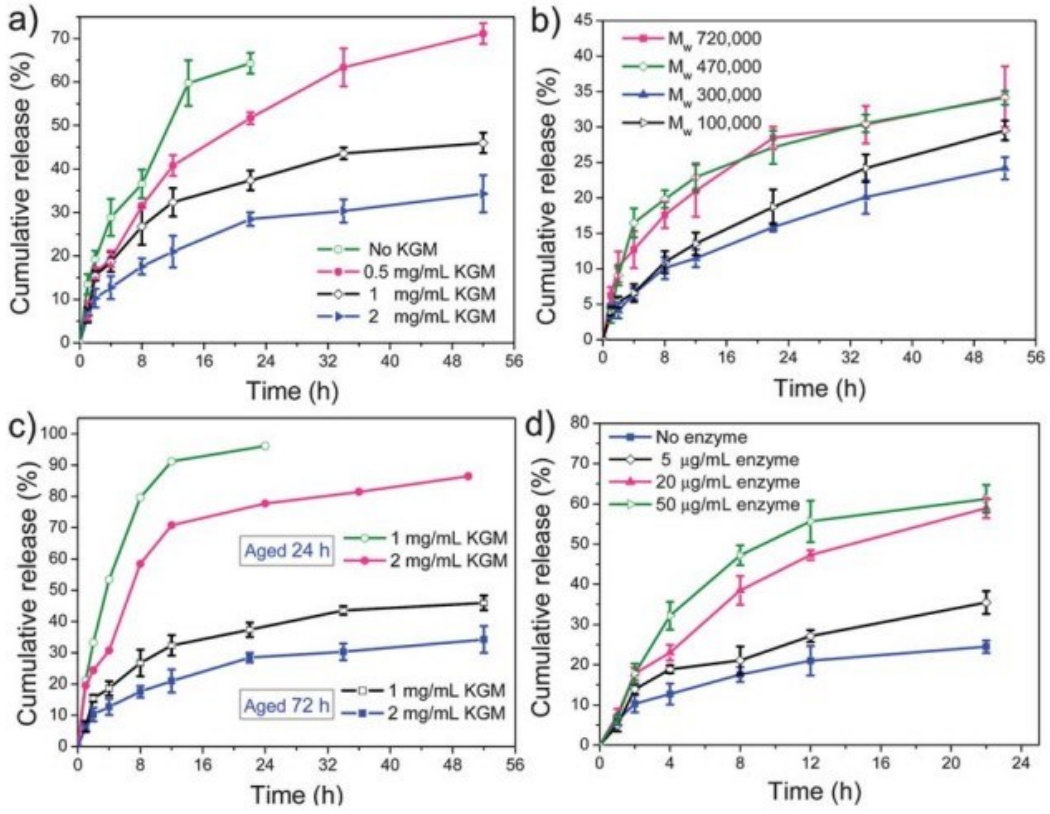

Figure 30. Graphs depicting the cumulative release of docetaxel from the drug-loaded Fmoc-FF peptide hydrogel and Fmoc-FF-KGM hybrid hydrogel at different a) KGM concentrations, b) KGM molecular weights, c) ageing times and d) β-mannanase concentrations in the release medium. Unless otherwise stated, the other default conditions were as follows: 0.1 mg mL^{-1} docetaxel, 2 mg mL^{-1} Fmoc-FF peptide, 2 mg mL^{-1} KGM, ageing time of 3 days, the volume of hydrogel was 0.5 mL, 2 mL pH 7.4 phosphate buffer solution (PBS), 37 ºC, 50 rpm.[44] Used with permission of RSC, from Self-assembling peptide-polysaccharide hybrid hydrogel as a potential carrier for drug delivery, Huang, R.; Qi, W.; Feng, L.; Su, R.; He, Z., 7, 2011; permission conveyed through Copyright Clearance Center, Inc.

8 Summary

Peptides and proteins represent the most promising components for creating the next generation of advanced materials.[5] The most frequently reported approach to formulating a peptide-based hydrogel involves using a single native peptide to design these materials. However, it suffers from several limitations, such as poor mechanical properties. To generate new useful properties, the development of multicomponent peptide-based hydrogels appears to be a promising method.[19] Combining two or more peptide sequences enables the creation of novel materials that self-sort or co-assemble, exhibiting improved properties in stability and mechanical performance. The chemical nature of the chosen peptides and their ratio within a multicomponent gel significantly impact the gelation time, stiffness, and biocompatibility of the resulting hydrogel.[6]

These multicomponent systems are highly complex, often difficult to fully predict and characterize. Understanding both the primary and larger scale structures is crucial for the overall properties. This is also particularly important when designing materials for a specific purpose.[14] Several different techniques can be employed to study the structure of multicomponent gels. However, examples where the type of assembly has been proved both at the molecular level and also at the length scales of fibers and networks, are limited.[25]

Multicomponent gels offer new useful properties and functionalities in materials, including self-replication, strong mechanical properties, resilience to high stress, higher tunability of properties, efficient energy transfer, and high stability. These enhanced features provide an opportunity to develop more complex functional materials for various applications, such as drug delivery, tissue engineering, nanoreactor design, and optoelectronic materials.[11,46]

It is evident that significant improvement is needed in understanding of the design of self-sorted or co-assembled gels, and in comprehending the assembly across multiple length scales. Although progress in this field is still ongoing, the abundance and variety of well-known gelators provide a lot of flexibility when designing intricate multicomponent gel systems.

EXPERIMENTAL PART

1 Introduction

Nowadays, protected amino acids and dipeptides are commonly used as low molecular weight gelators (LMWG). Fluorenylmethoxycarbonyl (Fmoc) is a large aromatic group typically used to protect an amino acid or dipeptide at the N-terminus.[47] Through hydrophobic and π-π interactions, the Fmoc group serves as a powerful initiator to promote self-assembly and plays a key role in hydrogel formation (Figure 31). Fmoc-protected amino acids or dipeptides usually form nanofibres exhibiting β-sheet secondary structures that entangle into a thicker network.[48] The fibers have a diameter of several tens of nanometers and a length of several microns.[47] Such hydrogels have numerous applications in the biomedical field, such as soft tissue engineering, drug delivery, cell encapsulation and cell growth.[49]

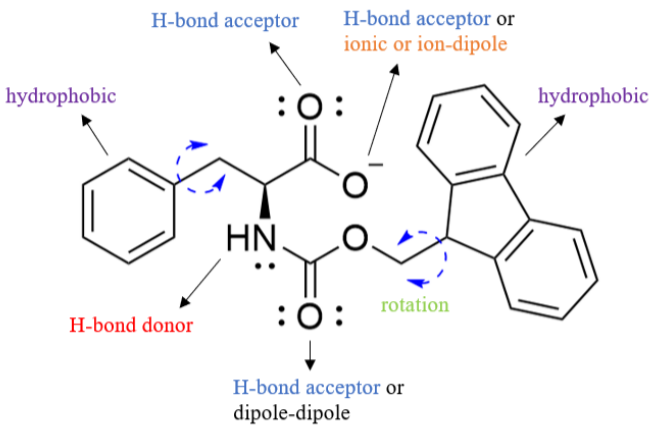

Figure 31. Potential sites of interactions in Fmoc-phenylalanine molecule.

Studies have focused on developing supramolecular systems in which two molecules non-covalently interact to form a fibrous network. Various possible assemblies can emerge, assuming that the interactions between the components are created by complementary chemical

groups. LMWG molecules self-assemble into one-dimensional fibers by self-sorting or co-assembling, depending on the preparation method or hydrophobicity. [49]

This project was based on a former study by Irwansyah *et al.*[50], who investigated the antimicrobial activity of a hydrogel containing Fmoc-F and Fmoc-Leucine (L). Fmoc-F and Fmoc-L are molecules consisting of a Fmoc protective group covalently bonded to phenylalanine and leucine, respectively (Figure 32).[51] The aim of this study was to investigate the formation of a two-component gel containing both molecules, the structure of the resulting gel fibers (whether self-sorting or co-assembly) and whether Fmoc-L participates in gel network formation. In addition, the effect of the ratio between the molecules on the structure of the gel network was studied. ^{1}H NMR spectroscopy and fluorescence measurements were used to investigate the participation of Fmoc-L in the gel formation, while FTIR spectroscopy was employed to investigate the secondary structures of the gel. In addition, AFM images were recorded to investigate the feasibility of gel deposition on a gold substrate for subsequent sSNOM measurements. Phase transition temperatures were also measured to assess whether differences arise in the macroscopic properties of the gels.

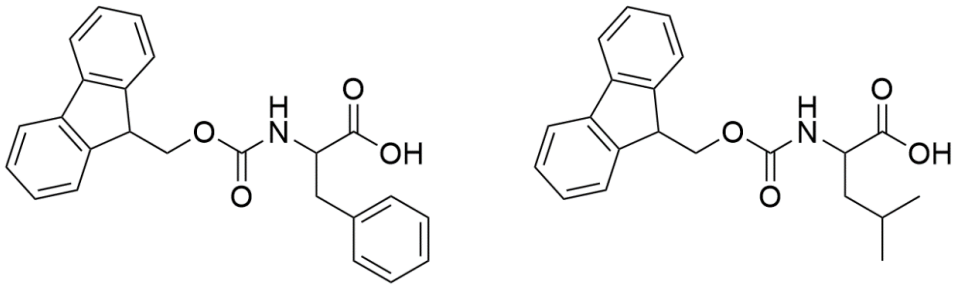

Fmoc-F **Fmoc-L**

Figure 32. Chemical structures of Fmoc-F and Fmoc-L molecules.

2 Materials and methods

All chemicals (Table 2) were used as received. The list of equipment used in this study is listed below.

Table 2. Manufacturers and purities of the used chemicals.

Chemical	Manufacturer	Purity
Sodium carbonate (Na_2CO_3)	Riedel-de Haën	99.8
N-[(9H-Fluoren-9-ylmethoxy)-carbonyl]-L-phenylalanine	TCI	> 98.0
N-[(9H-Fluoren-9-ylmethoxy)-carbonyl]-L-leucine	TCI	> 98.0
Phosphate Buffered Saline (PBS) tablets	Fisher Chemical	
Acetonitrile	Fisher Chemical	>= 99.0
D_2O	-	-

AFM imaging: Bruker Dimension Icon microscope in PeakForce tapping mode with Scan-Asyst-AIR probes (Bruker, USA) was used for AFM imaging.

Fluorescence: Varian Cary Eclipse fluorescence spectrophotometer was used to measure the fluorescence spectra of the gels in a quartz cuvette (path length: 1 cm, excitation wavelength: 289 nm, spectral range: 300 - 600 nm).

FT-IR: Bruker Tensor 27 FTIR spectrometer was used to measure the FT-IR spectra of the gels (spectral range: 400 - 4000 cm^{-1}, resolution: 4 cm^{-1}). 124 scans were taken for both background and sample.

NMR: ^1H NMR spectra were recorded with Bruker Advance III HD 500 MHz NMR-spectrometer. D_2O was used as a solvent and reference (δ_{D2O} = 4.79 ppm).

Scale: A Mettler Toledo XP205 scale was used to weigh Fmoc-amino acids.

UV/vis: UV/vis spectra were recorded with a Perkin Elmer Lambda 650 UV/VIS spectrometer in a quartz cuvette (path length: 10 mm).

3 Gelation experiments

A series of gels was prepared varying the ratio of Fmoc-F and Fmoc-L. Sodium carbonate solution (0.1 M) was added to the dry amino acids to dissolve them and to reach a molar ratio (F+L):Na_2CO_3 of 2:1 for every sample. The volume of solutions was adjusted to 1.0 mL with water. To enhance the solubility, solutions were sonicated and heated at 90 ºC for 1 h to 3 h). Hot solutions were allowed to cool slowly and undisturbed for at least 30 minutes. The gel formation was verified by the vial inversion method.

As a result, the lack of solubility in the sodium carbonate solution, long heating time (several hours) and the resulting high pH led to the change of solvent to Phosphate Buffered Saline (PBS) solution. Solutions were sonicated and heated at 80 ºC in a block heater (0.5 h-3 h). The hot solutions were allowed to cool undisturbed, and gelation was verified within five minutes by the vial inversion method (Figure 33).

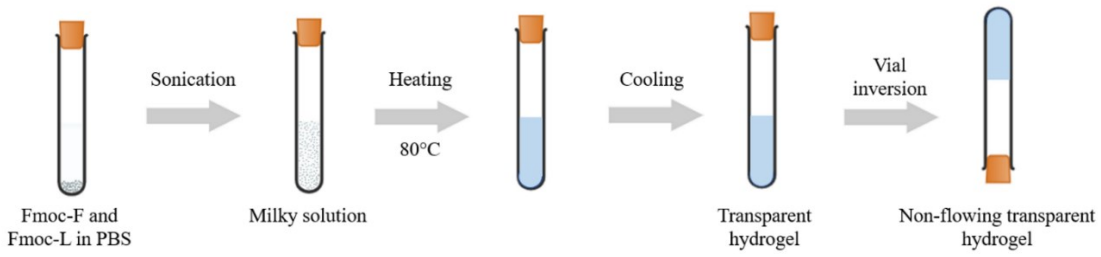

Figure 33. Gelation protocol with the heating-cooling method in PBS.

4 Results and discussion

4.1 Gelation results

Gels were prepared by varying the Fmoc-F: Fmoc-L ratio in two solvents (Na_2CO_3 and PBS). The results of the gelation trial in the sodium carbonate solution are shown in Table 3. Based on the literature, Fmoc-F is a known gelator in these conditions, while Fmoc-L is not. In our case, solutions in which the amount of Fmoc-F was higher than Fmoc-L formed a self-supporting gel, whereas the opposite conditions did not lead to the gel formation, therefore supporting the literature.

Table 3. Gelation outcome for Fmoc-F and Fmoc-L in carbonated solution.

Fmoc-F:Fmoc-L ratio	**Fmoc-F (mg)**	**Fmoc-L (mg)**	**0.1 M Na_2CO_3 (µL)**	**H_2O (µL)**	**Outcome**
1:0.2	10.00	1.82	155	845	SSG, transparent
1:0.4	10.00	3.65	181	819	SSG, transparent
1:0.6	10.00	5.47	206	794	SSG, transparent
1:0.8	10.00	7.30	232	768	SSG, particles
1:1	10.00	9.12	258	742	SSG, white particles
0.2:1	2.19	10.00	170	830	no SSG
0.4:1	4.38	10.00	198	802	no SSG
0.6:1	6.57	10.00	226	774	no SSG
0.8:1	8.77	10.00	255	745	no SSG

SSG = self-supporting gel

Due to the lack of solubility resulting in a long heating time and high pH value (7.6-7.9), the solvent was changed to PBS solution. The results for the gelation tests in PBS solution are shown in Table 4. Similarly to the carbonated solution, the samples containing a higher amount of Fmoc-F than Fmoc-L (**I-V**) formed a self-supporting gel, while the opposite conditions (**VI-IX**) either did not form a gel at all (**VI**) or only a weak gel (**VII-IX**, gel-like material that collapsed upon vial inversion). The gel systems (**I-IX**) are shown in Figure 34.

Gelation tests were also performed separately on Fmoc-F and Fmoc-L (2.00 mg/mL in PBS, identical protocol) to determine whether they are individually gelators. Only Fmoc-F formed a gel independently, while Fmoc-L did not. Therefore, the presence of Fmoc-F is required for gelation to occur. These results support the gelation trials presented in Figure 34 and Table 4.

Table 4. Gelation outcome for Fmoc-F and Fmoc-L in PBS solution.

Gel system	**Fmoc-F:Fmoc-L ratio**	**Fmoc-F (mg)**	**Fmoc-L (mg)**	**Outcome**
I	1 : 0.2	2.00	0.36	SSG, transparent
II	1 : 0.4	2.00	0.72	SSG, transparent
III	1: 0.6	2.00	1.10	SSG, transparent
IV	1 : 0.8	2.00	1.46	SSG, particles
V	1 : 1	2.00	1.82	SSG, particles
VI	0.2 : 1	0.44	2.00	no gel
VII	0.4 : 1	0.88	2.00	weak gel
VIII	0.6 : 1	1.32	2.00	weak gel
IX	0.8 :1	1.76	2.00	weak gel

SSG = self-supporting gel

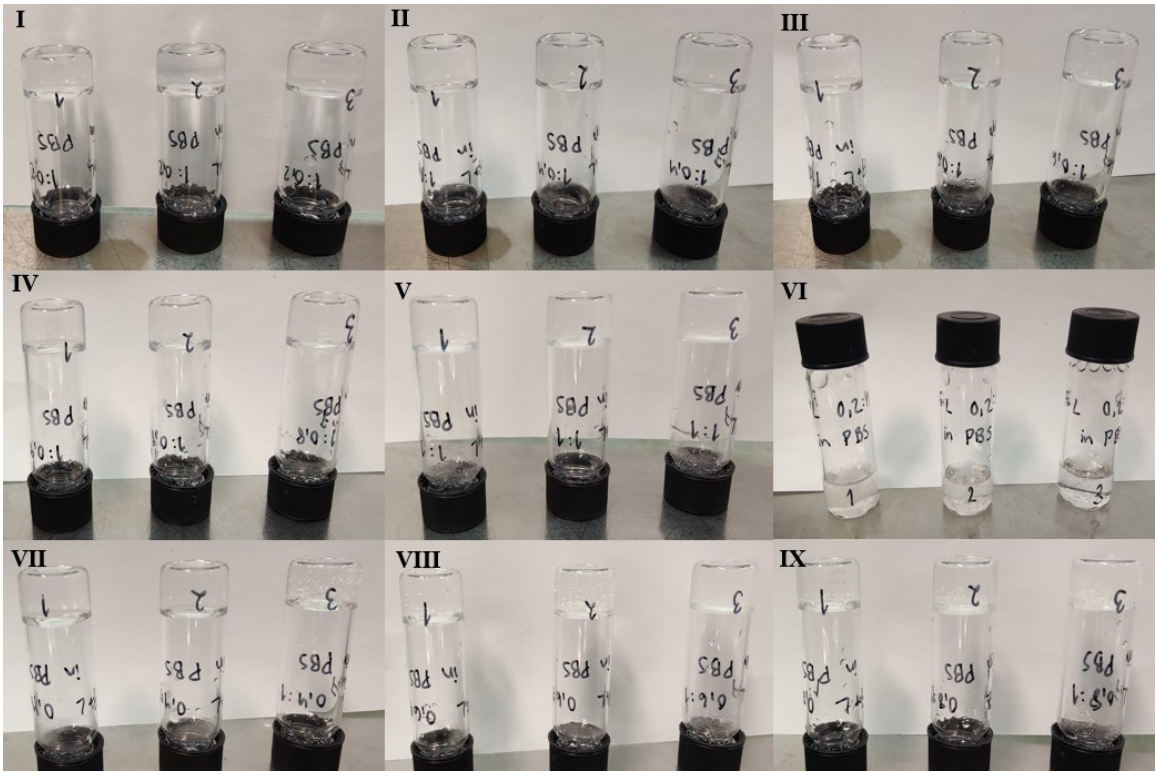

Figure 34. Vial inversion of the gel specimen **I**-**IX**.

4.2 Fourier-transform infrared (FT-IR) spectroscopy

Fourier-transform infrared spectroscopy (FT-IR) is widely used to provide information on the secondary structure of proteins. The sample is irradiated by infrared light, and the resulting spectrum gives insights into the functional groups present in the molecules, as well as conformations and foldings (α-helices, β-sheets).[52,53] The amide I band (1700-1600 cm^{-1}) is the spectral region where protein secondary structures are observed. The bands originate from the C=O stretching vibration of the peptide bonds and are the sum of individual structures (α-helices, β-sheets, turns and random structures).[53]

The gels were dried overnight in the open air, and the FT-IR spectra (gels **I**-**V**) were collected from 4000 cm^{-1} to 400 cm^{-1} (Figure 35). For all gel samples, a peak is observed between 1695 cm^{-1} and 1691 cm^{-1}, corresponding to β-sheet secondary structure[53]. In addition, shoulder peaks appear between 1682 cm^{-1} and 1676 cm^{-1}, which also correspond to β-sheet structures.[54]

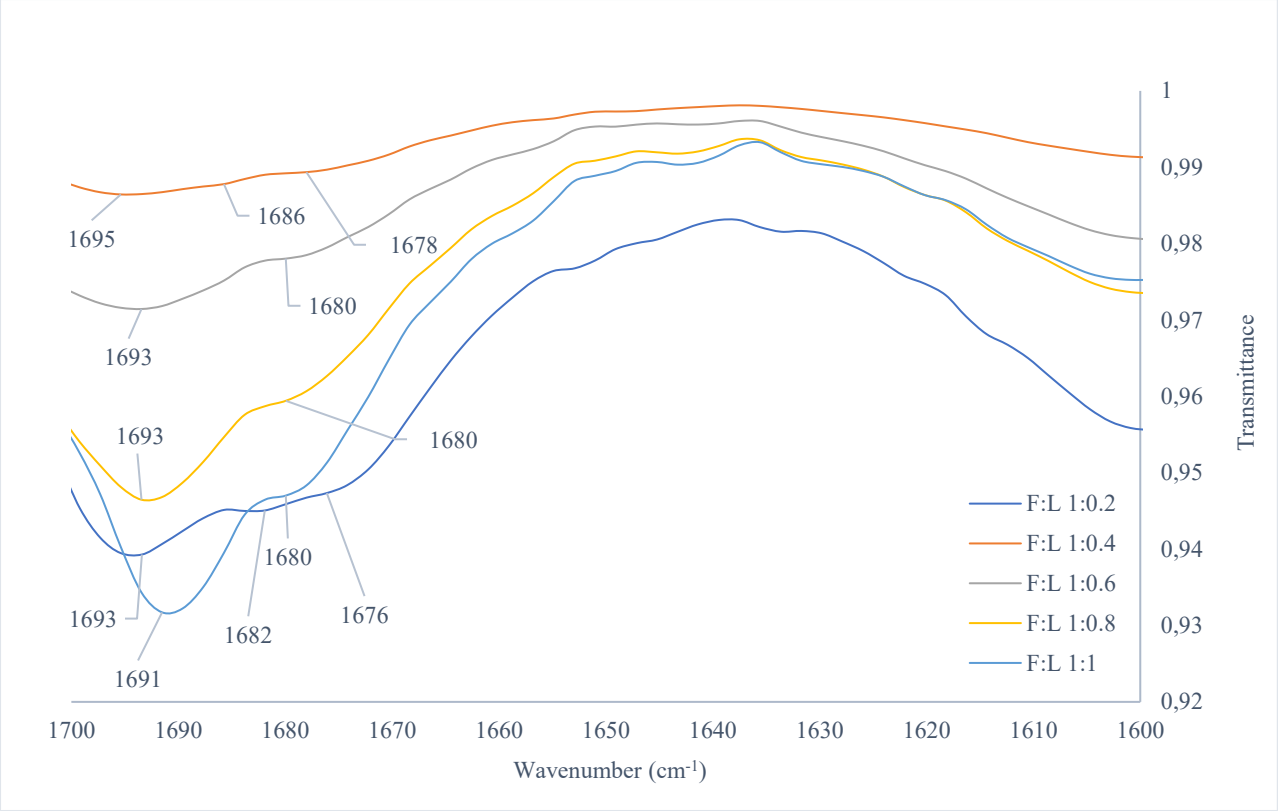

Figure 35. FT-IR spectrum of gels **I-V** in the amide I region 1700-1600 cm^{-1}.

The FT-IR spectra of gels **I-V** in the range 1200 to 1650 cm^{-1} are presented in Figure 36. The absorption within the amide II region (1480-1575 cm^{-1}) is mainly due to the N-H bending (here 1533 cm^{-1}).[52,53] The amide III region (1175-1310 cm^{-1}), showing a peak around 1254 cm^{-1}, is mainly related to CN stretching (~30 %), NH bending (~30 %), CC stretching (~20 %) and CH bending (~10 %) vibrations. This region is also sensitive to the secondary structures of protein, although its intensity is about five times lower than amide I.[55]

The small peaks at 1497 cm^{-1} and 1597 cm^{-1} correspond to the C=C stretching vibration of the aromatic ring of the phenylalanine moiety, whereas the peak at 1448 cm^{-1} corresponds to the C-H bending of the CH_3 in the leucine motif.[56]

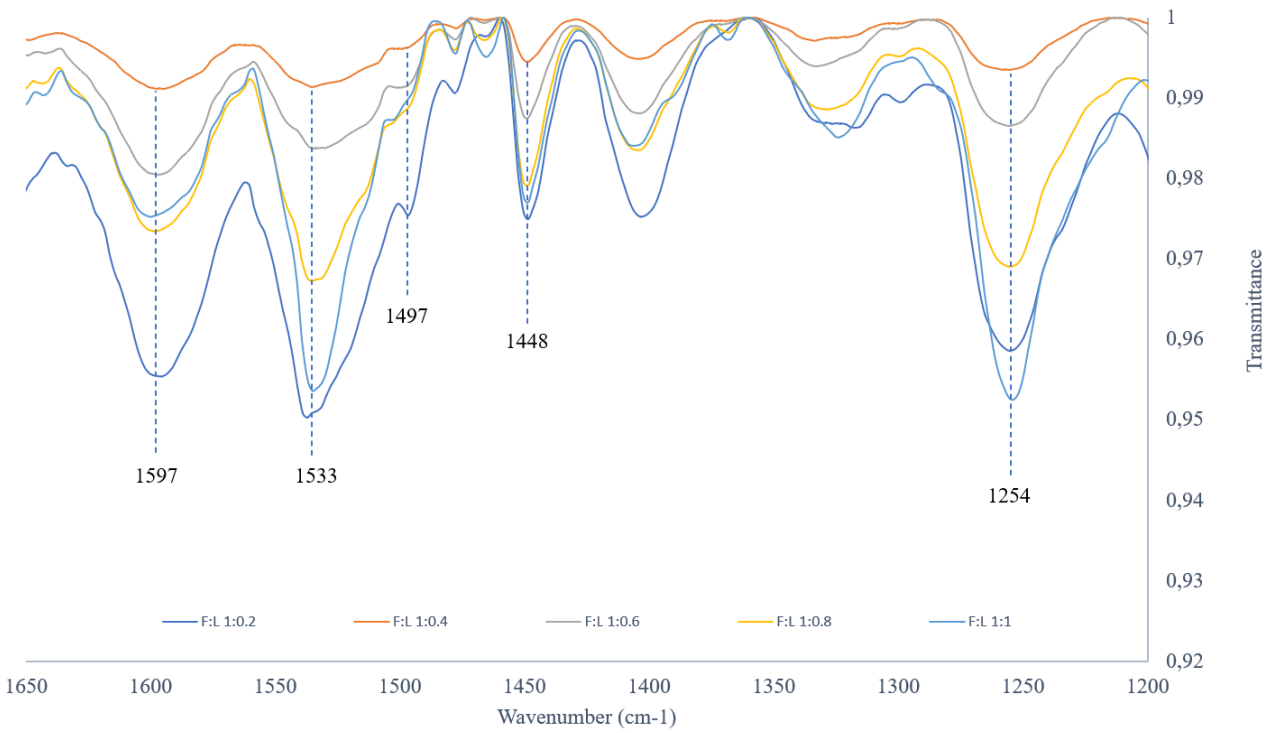

Figure 36. FT-IR spectrum of gels **I-V** in the range 1650-1200 cm^{-1}.

The spectra of all gels are quite similar, and there are no remarkable differences in the peak positions. This suggests that all gel systems have a similar composition regardless of their Fmoc-F:Fmoc-L ratios.

4.3 Phase transition temperature ($T_{gel\text{-}sol}$) measurements

Gels **I-V** were used for $T_{gel\text{-}sol}$ measurements and heated in a block heater. The initial temperature was 30 ºC and increased by 5 ºC every five minutes. The gels were left for 10 min at each temperature before checking with the vial inversion.

For gels **I-IV**, the $T_{gel\text{-}sol}$ was quantitatively similar (Table 5), whereas for gel **V**, the observed $T_{gel\text{-}sol}$ was significantly lower. This is presumably due to the high amount of insoluble Fmoc amino acids in the gel, resulting in a weaker gel.

Table 5. $T_{gel\text{-}sol}$ measurements for gels **I-V**.

Gel	**$T_{gel\text{-}sol}$ (°C)**
I	55-60
II	60-65
III	60-65
IV	60-65
V	30-35

All gels **I-V** are thermally reversible i.e. they formed a gel again after cooling (Figure 37). Interestingly, gels **II** and **III** turned opaque, suggesting a rearrangement of the network upon cooling.

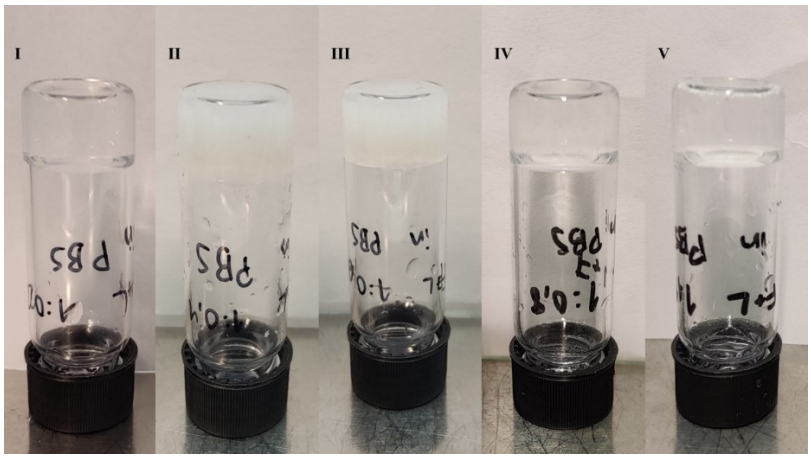

Figure 37. Gels **I-V** after $T_{gel\text{-}sol}$ measurements and cooling.

4.4 ^{1}H NMR

Nuclear Magnetic Resonance (NMR) can be a suitable method for monitoring the gelation process. Indeed, the gelator peaks are sharp and observable before the assembly broadens them upon fiber formation, and they become NMR invisible[2] due to the constraints on the free molecular rotation.

^{1}H NMR spectra of gels **I**-**V**, Fmoc-F (2 mg/mL; poor quality due to instrument maintenance and lack of time) and Fmoc-L (2.00 mg/mL and 0.36 mg/mL) in D2O solution were measured (Appendices 1-3) to observe the involvement of the leucine motif in the gel network formation. All samples were prepared in a deuterated PBS solution, and the NMR spectrum of the D2O solvent itself was measured to characterize potential solvent impurities (Appendix 4). There were quite a lot of impurities in the solvent and the ^{1}H NMR measurements should have been done again with new samples, but this was not done due to equipment failure and running out of time.

The ^{1}H NMR spectra of the gels **I**-**V** are shown in Figure 38. The spectra of the gels **II**-**V** have a broad peak at ~0.83 ppm, which originates from the leucine moiety in Fmoc-L. This suggests that part of Fmoc-L is in solution in the gel sample and, thus, potentially partially participates in forming the gel network. In gel **I**, this peak is not visible because the amount of Fmoc-L in the sample is so low. This is further verified by the spectrum of a sample containing only 0.36 mg/mL Fmoc-L (Appendix 3). Apart from solvent and impurities, no other peaks are visible in the spectrum of gel **I**, meaning that all Fmoc-F was involved in supramolecular interactions.

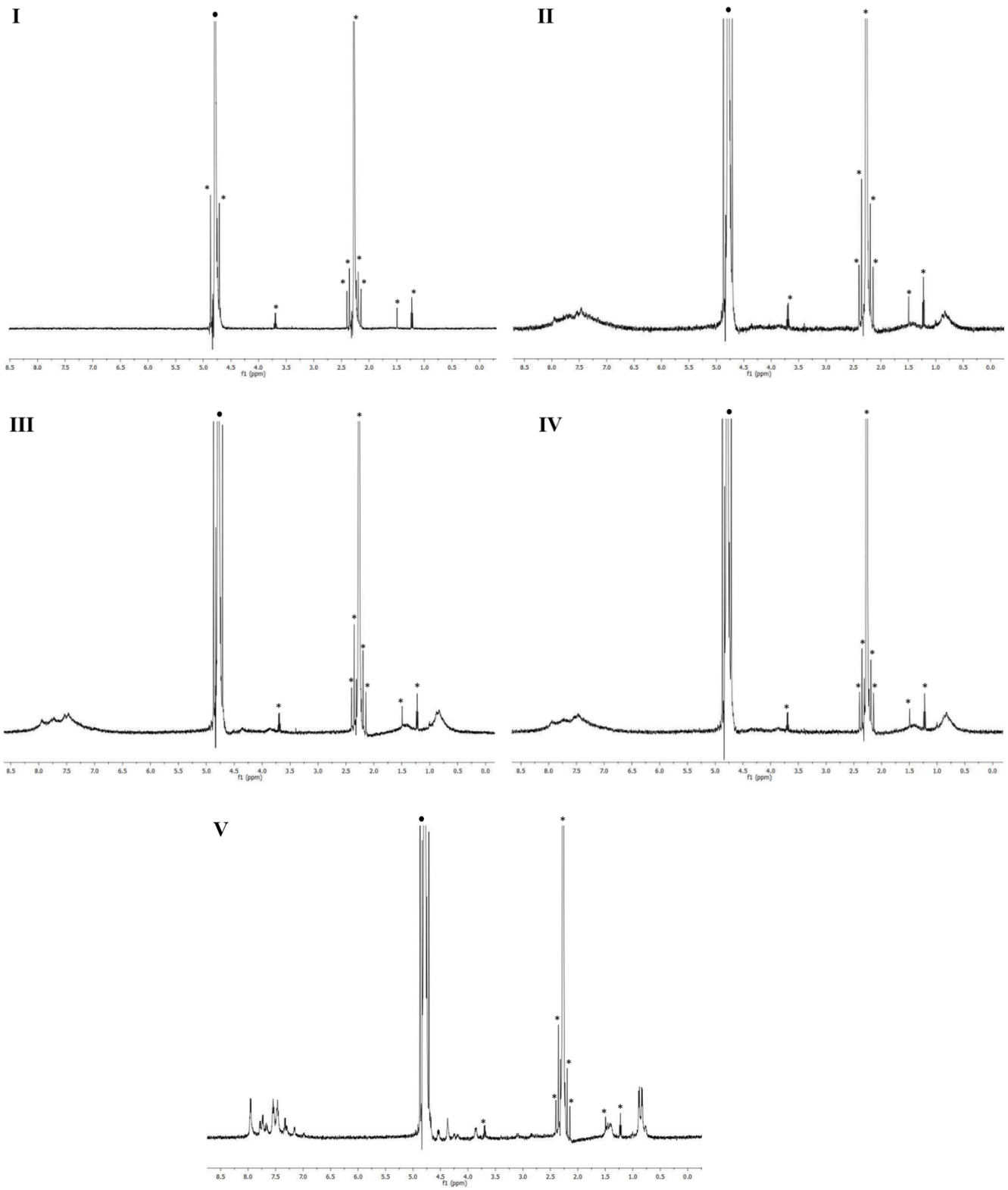

Figure 38. ^{1}H NMR spectra of gels **I**-**V**. Peaks marked with an asterisk indicate solvent impurities. Peaks marked with a dot at 4.79 ppm indicate the D_2O solvent.

The region of the aromatic protons is shown in Figure 39.[51] The complete loss of spectral features was observed in gel **I**, whereas for gels **II**-**IV**, a broad peak was observed, suggesting that some gelators are in the solution phase in the gel. However, in the spectrum of gel **V**, all the peaks appear sharp. The spectra were recorded at 30 ºC, and the $T_{gel\text{-}sol}$ measurements revealed that the gel-to-sol transition of gel **V** is 30-35 ºC. Therefore, gel **V** turned back to the solution during the measurement.

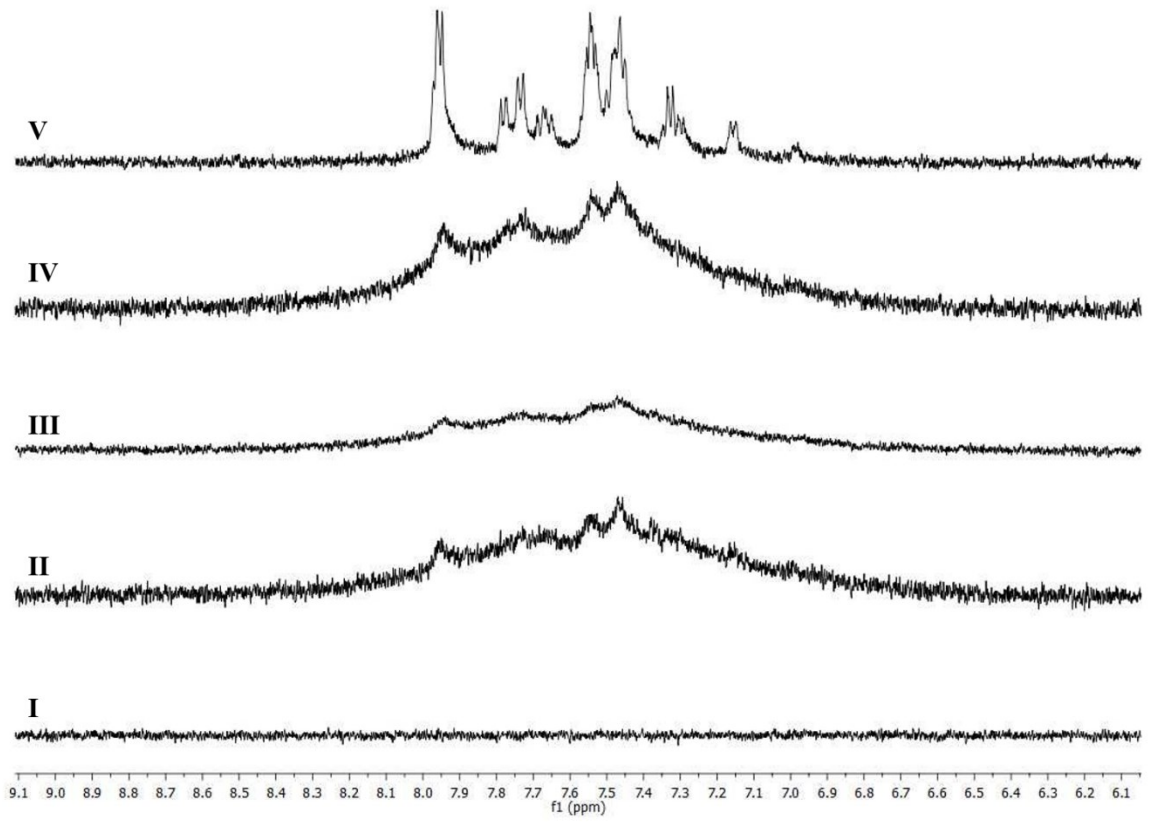

Figure 39. Aromatic proton region in the ^{1}H spectra of the gel samples **I**-**V**.

4.5 UV/vis and fluorescence

4.5.1 UV/vis measurements

For UV/vis measurements, Fmoc-F and Fmoc-L samples were prepared seperately by dissolving 0.5 mg of each amino acid in 5.0 mL of ACN. The samples were then diluted 20-fold to achieve a concentration of 0.005 mg/mL.

The UV/Vis spectra of Fmoc-F and Fmoc-L dissolved in ACN are presented in Figure 40. A broad peak at 265 nm and two smaller peaks at 289 and 299 nm are observed, corresponding to the π-π* transitions of the aromatic and fluorenyl groups,[57] respectively. No changes in the absorption band are observed depending on the amino acid attached to the Fmoc group. They are, therefore, not differentiable. Based on these measurements, 289 nm was chosen as the excitation wavelength for subsequent fluorescence measurements. The wavelength at 299 nm could possibly overlap with the fluorescence peak due to the small stoke shift of these gelator molecules.[58]

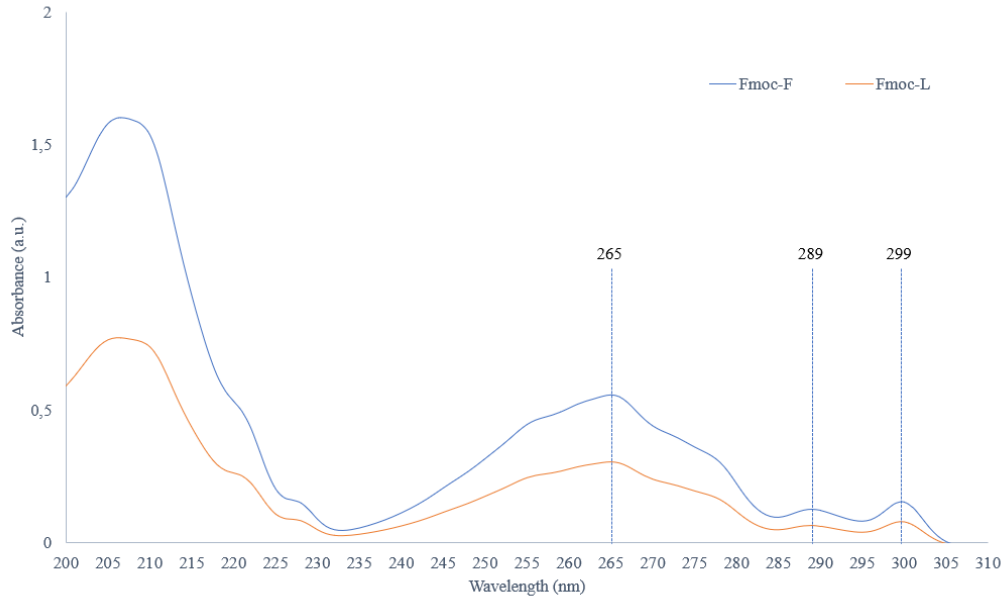

Figure 40. UV/vis-spectrum of Fmoc-F and Fmoc-L in ACN.

4.5.2 Fluorescence measurements

Fmoc-protected molecules are prone to aromatic interactions between the π-systems of the fluorenyl moieties, which play an important role in hydrogel formation.[59] Fluorescence spectroscopy was used to probe the molecular packing of the gelators and the potential role of Fmoc-L in the self-assembly.

For fluorescence measurements, gels **I**-**V** were prepared. Gels were prepared as in Table 4 but in three times the amount. Fmoc-F and Fmoc-L solution samples were the same as in UV/vis measurements. The solutions of Fmoc-F and Fmoc-L show a peak in the emission spectrum with a maximum intensity at 315 nm and 313, respectively (Figure 41). The intensity maximum of the gel samples appears at 319 nm (**I**, **IV** and **V**) and 322 nm (**II** and **III**). The intensity maximum of the hydrogels is red-shifted by 4 to 7 nm compared to the solution of Fmoc-F and 6-9 nm compared to the solution of Fmoc-L. The increase in dielectric constant around each fluorenyl chromophore and the transition from the free molecules of the solution phase to a more aggregated and organized molecular structure in the gel phase is responsible for the redshift of the emission maximum. This shift to 319 nm and 322 nm indicates an antiparallel arrangement of the Fmoc-F fluorenyl moieties.[59,60] A weak shoulder around 392 nm is also observed in the spectrum of the gels. This suggests that a small number of fluorenyl groups can also self-assemble in a parallel orientation.[59] A broad peak with a maximum at 458 nm in the gel emission spectrum is also observed, likely due to the formation of fluorenyl excimer species.[60]

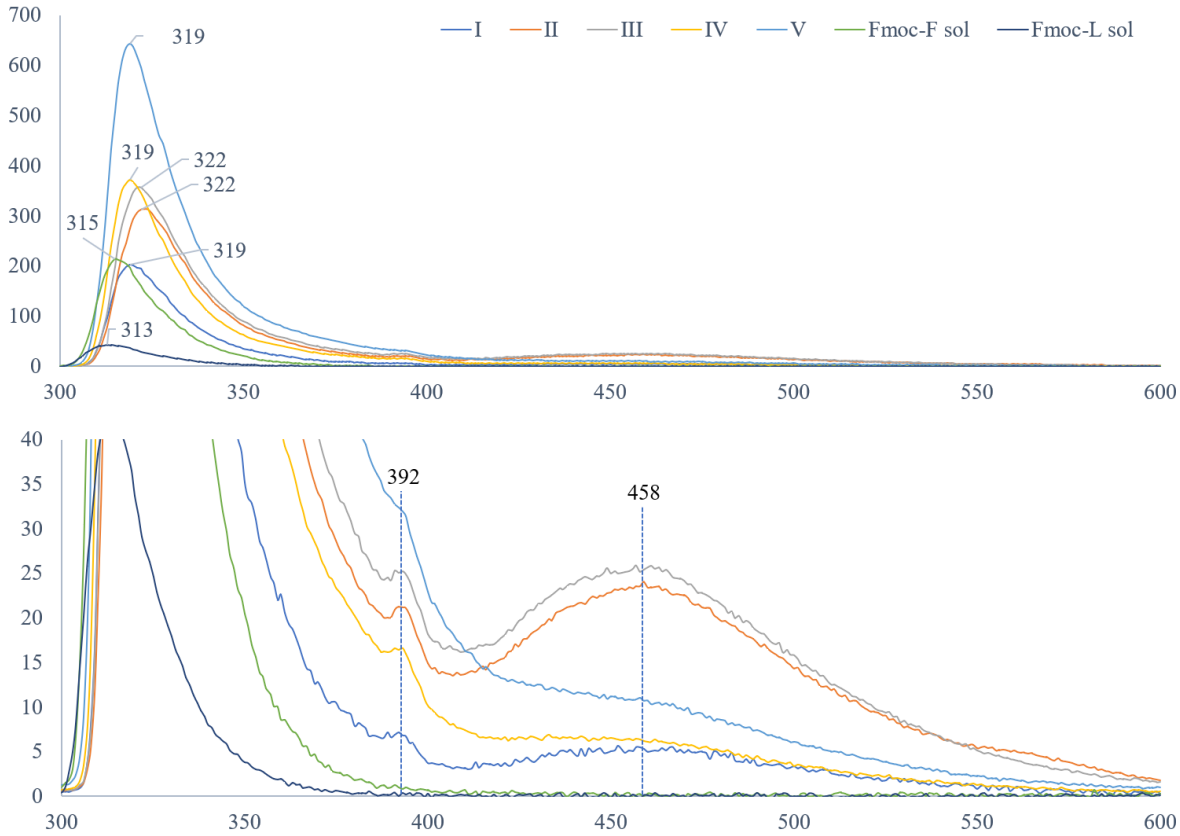

Figure 41. Fluorescence emission spectrum for Fmoc-F and Fmoc-L in solution and the gels **I**-**V**. Below is an enlargement of the upper spectrum to see the peaks at wavelengths 392 and 548.

Figure 42 shows that the fluorescence emission spectrum of the neat Fmoc-F gel and the dual component gel (Fmoc-F and Fmoc-L) are identical. Therefore, it can be stated that Fmoc-L does not participate in the formation of the gel network.

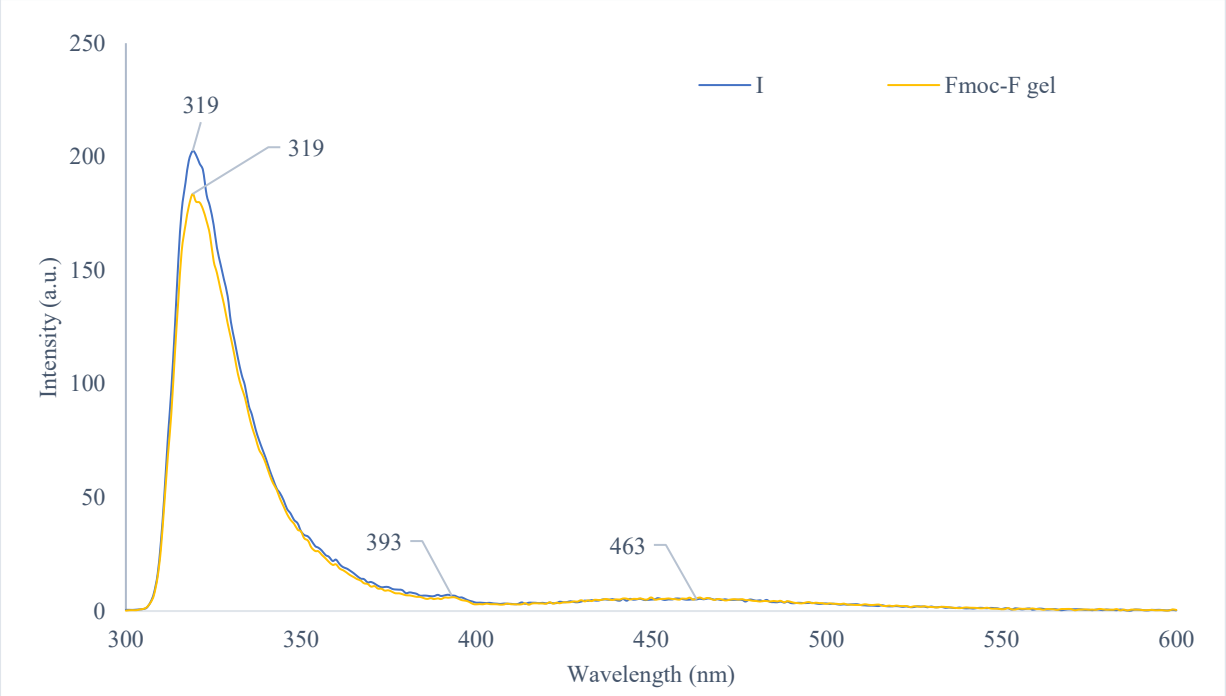

Figure 42. Fluorescence emission spectrum for Fmoc-F gel (2 mg/mL) and gel **I**.

4.5.3 Inner Filter Effect

Fluorescence measurements are also affected by the Inner Filter Effect (IFE), which occurs in the sample during the irradiation process. There are two types of IFE, both caused by the absorptive properties of the molecules. Type I IFE is always present and is due to Beer-Lambert's law. Type II IFE, also known as reabsorption, changes the shape of the fluorescence spectrum if the absorption and fluorescence spectra of the sample overlap. Indeed, the emitted light after excitation is partially reabsorbed by the sample.[61]

This effect was evaluated using a concentration series of Fmoc-F solutions (0.5 mg/mL, 1.0 mg/mL, 1.5 mg/mL and 2.0 mg/mL). Measuring different concentrations ensured that the IFE did not affect the previous conclusion based on the fluorescence peak shifts. As shown in Figure 43, the intensity maxima do not shift when varying the sample concentration. Therefore, it is assumed that the IFE is minor and negligible.

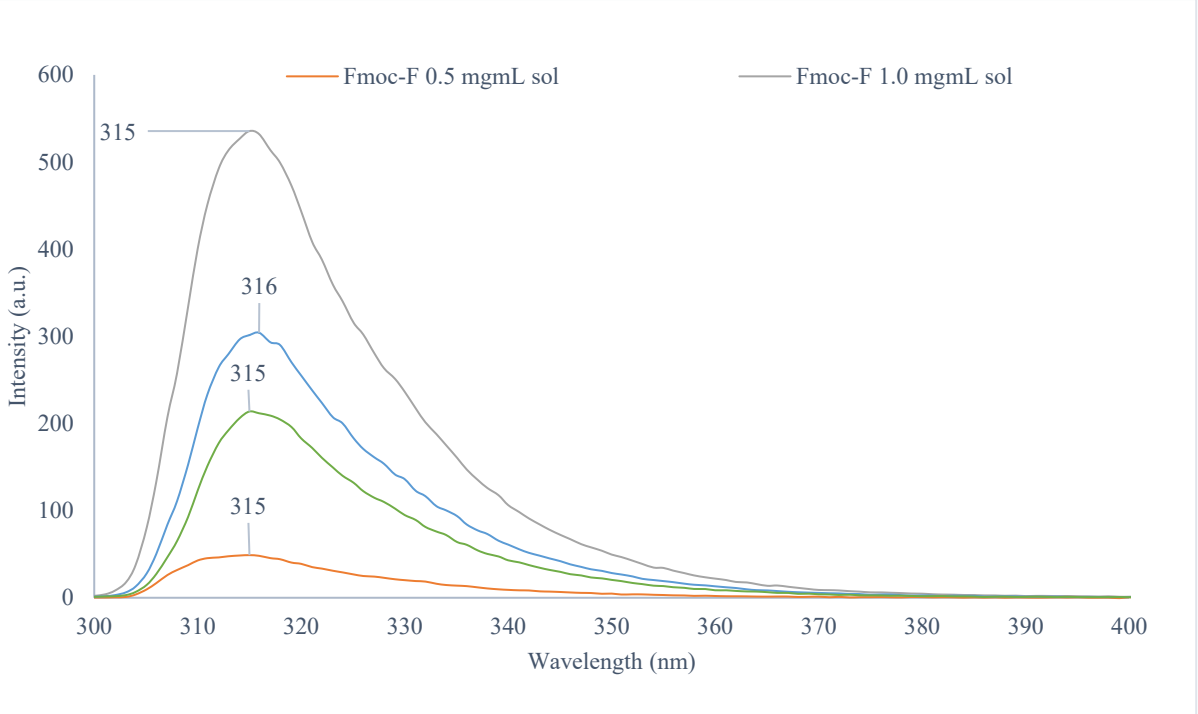

Figure 43. Fluorescence spectra of Fmoc-F solutions from concentrations 0.5 mg/mL, 1.0 mg/mL, 1.5 mg/mL and 2.0 mg/mL to study the inner filter effect.

4.6 Atomic force microscope (AFM) imaging

AFM imaging was performed to find the suitable sample preparation procedure (deposition, drying, rotation speed and duration) for future sSNOM experiments. An attempt was first made to prepare a sample for SNOM analysis from gel **I** by pipetting 1 µl of the hot solution onto Au coated silicon chip. Gelation was allowed to occur in the chamber illustrated in Figure 44. After gelation, the sample was dried in a freeze dryer. Due to the high surface tension between the water and Au surface, the direct pipetting of the solution onto the chip yielded a too dense network of fibers. To solve this problem, spin coating was used to prepare the sample because it would spread the solution droplet more evenly on the surface.

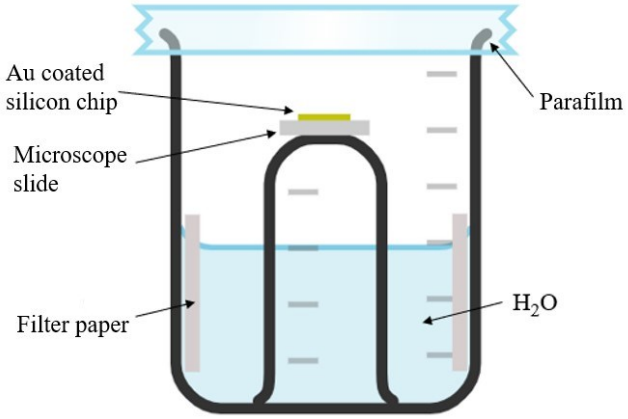

Figure 44. The first method that was attempted to make samples for SNOM analysis.

Images were then recorded on gel **I** deposited on Au-coated Si chips. Samples were prepared by spin coating while varying parameters such as rotation speed and duration (Table 6). The hot gel solution was pipetted onto the chip, and gelation took place during cooling in the spin coater.

Table 6. Rotation speeds and times on Au-coated chips.

Sample	Rotation speed (rpm)	Rotation time (s)
A	500	5
B	500	30
C	500	30
D	1000	30
E	1750	30
F	2500	30

The AFM images of the samples **B**-**F** (Figure 45) are taken from the less dense areas (black square). A high-resolution image could not be recorded on sample **A** due to the dense network

all over the sample, probably arising from the short rotation time. Samples **B** and **C** had a similar rotation speed but a longer rotation time, which led to more spread fibres. For the other samples with a higher rotation speed (**D** to **F**), no significant differences were observed. Therefore, 500 rpm and 30 s were found to be the best conditions for sample preparation. Unfortunately, sSNOM measurements could not be performed due to equipment maintenance.

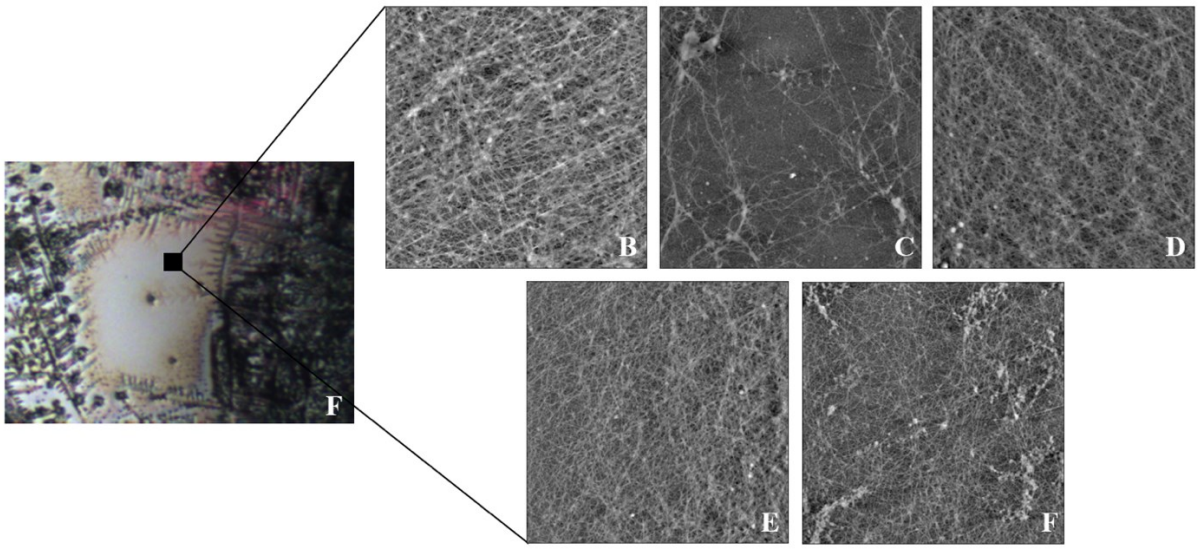

Figure 45. AFM images (5 µm x 5 µm) of gel **I** from samples **B**-**F**.

5 Conclusion

The purpose of this study was to prepare a two-component hydrogel containing Fmoc-F and Fmoc-L in PBS solution to assess the molecular packing and the gel fiber formation and to observe whether self-sorting or co-assembly occurred. In addition, the structure of the gel depending on the ratios of Fmoc-F and Fmoc-L was studied.

^{1}H NMR spectroscopy and fluorescence measurements revealed that Fmoc-L weakly participates in the formation of the gel network. This indicates that the gel fibers are mostly formed via the self-sorting of Fmoc-F molecules. Fluorescence measurements also revealed that most of the Fmoc-F fluorenyl moieties are arranged antiparallel, with a small part also arranged parallel. In addition, the formation of fluorenyl excimer species was observed. FT-IR spectroscopy showed that the secondary structures of the gels are similar and contain β-sheet structures, regardless of the ratio.

Originally, analysis of the gels by sSNOM was assumed to give insights into the participation of Fmoc-L in the fibre formation. However, this experiment remains to be performed in the future. Spin coating was found to be a good method for preparing samples on Au coated silicon chips and the samples imaged by AFM are suitable for SNOM studies.

During the conduction of the research, dissolution issues arose with the amino acids. In the future, solubility tests could be performed, and other solvent options could be considered to address these issues. In the continuation of this the research, the ^{1}H NMR measurements should be repeated with new samples, as the spectra obtained in this study were of poor quality and the solvent contained a lot of impurities. The weak gelator component, in this study Fmoc-L, is generally proven to affect the bulk properties of the gel by affecting nucleation and fiber growth.[3] The research could be carried out to determine how Fmoc-L affects these properties on the gels.

References

1. Buerkle, L. E. and Rowan, S. J., Supramolecular gels formed from multi-component low molecular weight species, *Chem. Soc. Rev.*, **2012**, *41*, 6089–6102.
2. Draper, E. R. and Adams, D. J., How should multicomponent supramolecular gels be characterised?, *Chem. Soc. Rev.*, **2018**, *47*, 3395–3405.
3. Panja, S.; Dietrich, B.; Smith, A. J.; Seddon, A. and Adams, D. J., Controlling Self-Sorting versus Co-assembly in Supramolecular Gels, *ChemSystemsChem*, **2022**, *4*, e202200008.
4. Li, L.; Sun, R. and Zheng, R., Tunable morphology and functionality of multicomponent self-assembly: A review, *Mater. Des.*, **2021**, *197*, 109209.
5. Okesola, B. O. and Mata, A., Multicomponent self-assembly as a tool to harness new properties from peptides and proteins in material design, *Chem. Soc. Rev.*, **2018**, *47*, 3721–3736.
6. Diaferia, C.; Ghosh, M.; Sibillano, T.; Gallo, E.; Stornaiuolo, M.; Giannini, C.; Morelli, G.; Adler-Abramovich, L. and Accardo, A., Fmoc-FF and hexapeptide-based multicomponent hydrogels as scaffold materials, *Soft Matter.*, **2019**, *15*, 487–496.
7. Christoff-Tempesta, T., Lew, A. J., Ortony, J. H., Beyond Covalent Crosslinks: Applications of Supramolecular Gels, *Gels*, **2018**, *4(2)*, 40.
8. Pramanik, B., Ahmed, S., Peptide-Based Low Molecular Weight Photosensitive Supramolecular Gelators, *Gels*, **2022**, *8(9)*, 533.
9. Chu, C.-W. and Schalley, C. A., Recent Advances on Supramolecular Gels: From Stimuli-Responsive Gels to Co-Assembled and Self-Sorted Systems, *Org. Mater.*, **2021**, *03*, 025–040.
10. A, C. P. R.; Smith, D. K. and Link to external site, Shaping and structuring supramolecular gels, *Nat. Rev. Mater.*, **2019**, *4*, 463–478.
11. Falcone, N.; Shao, T.; Andoy, N. M. O.; Rashid, R.; Sullan, R. M. A.; Sun, X. and Kraatz, H.-B., Multi-component peptide hydrogels – a systematic study incorporating biomolecules for the exploration of diverse, tuneable biomaterials, *Biomater. Sci.*, **2020**, *8*, 5601–5614.
12. Giuri, D.; Marshall, L. J.; Dietrich, B.; McDowall, D.; Thomson, L.; Newton, J. Y.; Wilson, C.; Schweins, R. and Adams, D. J., Exploiting and controlling gel-to-crystal transitions in multicomponent supramolecular gels, *Chem. Sci.*, **2021**, *12*, 9720–9725.
13. Hirst, A. R. and Smith, D. K., Two-Component Gel-Phase Materials—Highly Tunable Self-Assembling Systems, *Chem. – Eur. J.*, **2005**, *11*, 5496–5508.

14. Randle, R. I.; Ginesi, R. E.; Matsarskaia, O.; Schweins, R. and Draper, E. R., Process Dependent Complexity in Multicomponent Gels, *Macromol. Rapid Commun.*, **2023**, *44*, 2200709.

15. Draper, E. R. and Adams D. J., Low-Molecular-Weight Gels: The State of the Art, *Chem*, **2017**, *3*, 390-410.

16. Marshall, L. J.; Bianco, S.; Ginesi, R. E.; Doutch, J.; Draper, E. R. and Adams, D. J., Investigating multigelator systems across multiple length scales, *Soft Matter*, **2023**, *19*, 4972–4981.

17. Loos, J. N.; D'Acierno, F.; Mody, U. V.; MacLachlan, M. J., Manipulating the Self-Assembly of Multicomponent Low Molecular Weight Gelators (LMWGs) through Molecular Design, *ChemPlusChem*, **2022**, *87*, e202200026.

18. Croitoriu, A.; Nita, L. E.; Chiriac, A. P.; Rusu, A. G. and Bercea, M., New Physical Hydrogels Based on Co-Assembling of FMOC–Amino Acids, *Gels*, **2021**, *7*, 208.

19. Giraud, T.; Bouguet-Bonnet, S.; Stébé, M.-J.; Richaudeau, L.; Pickaert, G.; Averlant-Petit, M.-C. and Stefan, L., Co-assembly and multicomponent hydrogel formation upon mixing nucleobase-containing peptides, *Nanoscale*, **2021**, *13*, 10566–10578.

20. Raymond, D. M. and Nilsson, B. L., Multicomponent peptide assemblies, *Chem. Soc. Rev.*, **2018**, *47*, 3659–3720.

21. Martin, A. D. and Thordarson, P., Beyond Fmoc: a review of aromatic peptide capping groups, *J. Mater. Chem. B*, **2020**, *8*, 863–877.

22. Diaferia, C.; Morelli, G. and Accardo, A., Fmoc-diphenylalanine as a suitable building block for the preparation of hybrid materials and their potential applications, *J. Mater. Chem. B*, **2019**, *7*, 5142–5155.

23. Baek, K.; Noblett, A. D.; Ren, P.; Suggs, L. J., Design and Characterization of Nucleopeptides for Hydrogel Self-Assembly, *ACS Appl. Bio Mater*., **2019**, *2*, 7, 2812-2821.

24. Ray, A. and Nordén, B., Peptide nucleic acid (PNA): its medical and biotechnical applications and promise for the future, *FASEB J.*, **2000**, *14*, 1041–1060.

25. Raeburn, J. and Adams, D. J., Multicomponent low molecular weight gelators, *Chem. Commun.*, **2015**, *51*, 5170–5180.

26. Xing, P. and Zhao Y., Controlling Supramolecular Chirality in Multicomponent Self-Assembled Systems, *Acc. Chem. Res*., **2018**, *51*, 9, 2324-2334.

27. Zhang, L.; Qin, L.; Wang, X.; Cao, H. and Liu, M., Supramolecular Chirality in Self-Assembled Soft Materials: Regulation of Chiral Nanostructures and Chiral Functions, *Adv. Mater.*, **2014**, *26*, 6959–6964.

28. Tómasson, D. A.; Ghosh, D.; Kržišnik, Z.; Fasolin, L. H.; Vicente, A. A.; Martin, A. D.; Thordarson, P.; Damodaran, K. K., Enhanced Mechanical and Thermal Strength in Mixed-Enantiomers-Based Supramolecular Gel, *Langmuir*, **2018**, *34*, 43, 12957-12967.

29. Afrasiabi, R. and Kraatz H.-B., Small-Peptide-Based Organogel Kit: Towards the Development of Multicomponent Self-Sorting Organogels, *Chem. - Eur. J.*, **2013**, *19*, 47, 15862-15871.

30. Colquhoun, C.; Draper, E. R.; Eden, E. G. B.; Cattoz, B. N.; Morris, K. L.; Chen, L.; McDonald, T. O.; Terry, A. E.; Griffiths, P. C.; Serpell, L. C. and Adams, D. J., The effect of self-sorting and co-assembly on the mechanical properties of low molecular weight hydrogels, *Nanoscale*, **2014**, *6*, 13719–13725.

31. Ryan, D. M.; Doran, T. M.; Nilsson, B. L.; Complementary π–π Interactions Induce Multicomponent Coassembly into Functional Fibrils, *Langmuir*, **2011**, *27*, 17, 11145-11156.

32. Draper, E. R.; Lee, J. R.; Wallace, M.; Jäckel, F.; Cowan, A. J. and Adams, D. J., Self-sorted photoconductive xerogels, *Chem. Sci.*, **2016**, *7*, 6499–6505.

33. Ardoña, H. A. M.; Draper, E. R.; Citossi, F.; Wallace, M.; Serpell, L. C.; Adams, D. J.; Tovar, J. D., Kinetically Controlled Coassembly of Multichromophoric Peptide Hydrogelators and the Impacts on Energy Transport, *J. Am. Chem. Soc.*, **2017**, *139*, 25, 8685-8692.

34. Yu, G.; Yan, X.; Han, C. and Huang, F., Characterization of supramolecular gels, *Chem. Soc. Rev.*, **2013**, *42*, 6697-6722.

35. Jayawarna, V.; Ali, M.; Jowitt, T. A.; Miller, A. F.; Saiani, A.; Gough, J. E. and Ulijn, R. V., Nanostructured Hydrogels for Three-Dimensional Cell Culture Through Self-Assembly of Fluorenylmethoxycarbonyl–Dipeptides, *Adv. Mater.*, **2006**, *18*, 611–614.

36. Li, D.; Shi, Y. and Wang, L., Mechanical Reinforcement of Molecular Hydrogel by Co-assembly of Short Peptide-based Gelators with Different Aromatic Capping Groups, *Chin. J. Chem.*, **2014**, *32*, 123–127.

37. Moff*at, J. R.* and Smith, D. K., Controlled self-sorting in the assembly of 'multi-gelator' gels*, Chem. Commun.*, **2009,** 316-318.

38. Guilbaud, J.-B. and Saiani, A., Using small angle scattering (SAS) to structurally characterise peptide and protein self-assembled materials, *Chem. Soc. Rev.*, **2011**, *40*, 1200–1210.

39. Mears, L. L. E.; Draper, E. R.; Castilla, A. M.; Su, H.; Zhuola, Z.; Dietrich, B.; Nolan, M. C.; Smith, G. N.; Doutch, J.; Rogers, S.; Akhtar, R.; Cui, H.; Adams, D. J., Drying Affects

the Fiber Network in Low Molecular Weight Hydrogels, *Biomacromolecules*, *2017*, *18*, 11, 3531-3540.

40. McDowall, D.; Adams, D. J. and Seddon, A. M., Using small angle scattering to understand low molecular weight gels, *Soft Matter*, **2022**, *18*, 1577–1590.
41. Loos, J. N.; Boott, C. E.; Hayward, D. W.; Hum, G.; MacLachlan, M. J., Exploring the Tunable Optical and Mechanical Properties of Multicomponent Low-Molecular-Weight Gelators, *Langmuir*, **2021**, *37*, 1, 105-114.
42. Fichman, G.; Guterman, T.; Adler-Abramovich, L. and Gazit, E., Synergetic functional properties of two-component single amino acid-based hydrogels, *CrystEngComm*, **2015**, *17*, 8105–8112.
43. Ghosh, M.; Halperin-Sternfeld, M.; Grigoriants, I.; Lee, J.; Nam, K. T.; Alder-Abramovich, L., Arginine-Presenting Peptide Hydrogels Decorated with Hydroxyapatite as Biomimetic Scaffolds for Bone Regeneration, *Biomacromolecules*, **2017**, *18*, 11, 3541-3550.
44. Huang, R.; Qi, W.; Feng, L.; Su, R. and He, Z., Self-assembling peptide–polysaccharide hybrid hydrogel as a potential carrier for drug delivery, *Soft Matter*, **2011**, *7*, 6222-6230.
45. Jiang, M.; Li, H.; Shi, J. and Xu, Z., Depolymerized konjac glucomannan: preparation and application in health care, *J. Zhejiang Univ.-Sci. B*, **2018**, *19*, 505–514.
46. Okesola, B. O.; Wu, Y.; Derkus, B.; Gani, S.; Wu, D.; Knani, D.; Smith, D. K.; Adams, D. J. and Mata, A., Supramolecular Self-Assembly To Control Structural and Biological Properties of Multicomponent Hydrogels, *Chem. Mater.*, **2019**, *31*, 7883–7897.
47. Draper, E. R.; Morris, K. L.; Little, M. A.; Raeburn, J.; Colquhoun, C.; Cross, E. R.; McDonald, Tom. O.; Serpell, L. C. and Adams, D. J., Hydrogels formed from Fmoc amino acids, *CrystEngComm*, **2015**, *17*, 8047–8057.
48. Kang, J. and Yun, S. I., Fmoc-phenylalanine as a building block for hybrid double network hydrogels with enhanced mechanical properties, self-recovery, and shape memory capability, *Polymer*, **2022**, *255*, 125145.
49. Croitoriu, A.; Nita, L. E.; Rusu, A. G.; Ghilan, A.; Bercea, M. and Chiriac, A. P., New Fmoc-Amino Acids/Peptides-Based Supramolecular Gels Obtained through Co-Assembly Process: Preparation and Characterization, *Polymers*, **2022**, *14*, 3354.
50. Irwansyah, I.; Li, Y.-Q.; Shi, W.; Qi, D.; Leow, W. R.; Tang, M. B. Y.; Li, S. and Chen, X., Gram-Positive Antimicrobial Activity of Amino Acid-Based Hydrogels, *Adv. Mater.*, **2015**, *27*, 648–654.
51. Singh, V.; Snigdha, K.; Singh, C.; Sinha, N. and Thakur, A. K., Understanding the self-assembly of Fmoc–phenylalanine to hydrogel formation, *Soft Matter*, **2015**, *11*, 5353–5364.

52. Gallagher, W., FTIR Analysis of Protein Structure, *Course manual Chem*, **2009**, 455.

53. Kong, J. and You, S., Fourier Transform Infrared Spectroscopic Analysis of Protein Secondary Structures, *Acta Biochim. Biophys. Sin.*, **2007**, 549–559.

54. Barth, A., Infrared spectroscopy of proteins, *Biochim. Biophys. Acta BBA - Bioenerg.*, **2007**, *1767*, 1073–1101.

55. Stani, C.; Vaccari, L.; Mitri, E. and Birarda, G., FTIR investigation of the secondary structure of type I collagen: New insight into the amide III band, *Spectrochim. Acta. A. Mol. Biomol. Spectrosc.*, **2020**, *229*, 118006.

56. Barth, A., The infrared absorption of amino acid side chains, *Prog. Biophys. Mol. Biol.*, **2000**, *74*, 141–173.

57. Aguilera, J.; García-González, V.; Alatorre-Meda, M.; Rodríguez-Velázquez, E. and Rivero, I., Synthesis of BODIPY-Amino Acids and the Potential Applications as Specific Dyes for the Cytoplasm of Langerhans β-Cells, *J. Braz. Chem. Soc.*, **2021**, 2222-2234.

58. Zhou, R.; Lu, X.; Yang, Q. and Wu, P., Nanocrystals for large Stokes shift-based optosensing, *Chin. Chem. Lett.*, **2019**, *30*, 1843–1848.

59. Reddy, S. M. M.; Shanmugam, G.; Duraipandy, N.; Kiran, M. S. and Mandal, A. B., An additional fluorenylmethoxycarbonyl (Fmoc) moiety in di-Fmoc-functionalized L -lysine induces pH-controlled ambidextrous gelation with significant advantages, *Soft Matter*, **2015**, *11*, 8126–8140.

60. Ryan, K.; Beirne, J.; Redmond, G.; Kilpatrick, J. I.; Guyonnet, J.; Buchete, N.-V.; Kholkin, A. L. and Rodriguez, B. J., Nanoscale Piezoelectric Properties of Self-Assembled Fmoc–FF Peptide Fibrous Networks, *ACS Appl. Mater. Interfaces*, **2015**, *7*, 12702–12707.

61. Kasparek, A. and Smyk, B., A new approach to the old problem: Inner filter effect type I and II in fluorescence, *Spectrochim. Acta. A. Mol. Biomol. Spectrosc.*, **2018**, *198*, 297–303.

Appendices

APPENDIX 1

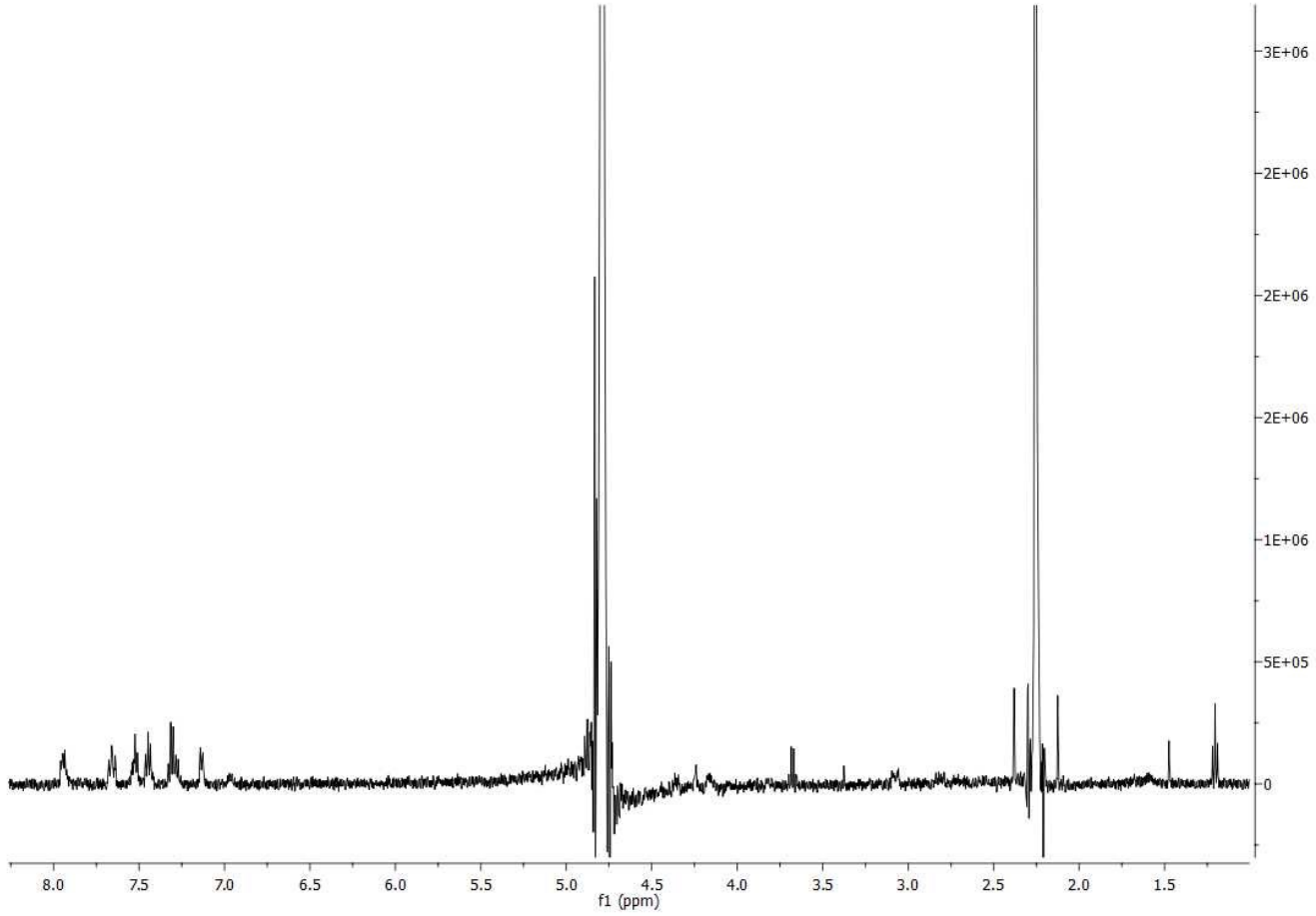

^{1}H NMR spectrum of Fmoc-F (2mg/mL) in D_2O

APPENDIX 2

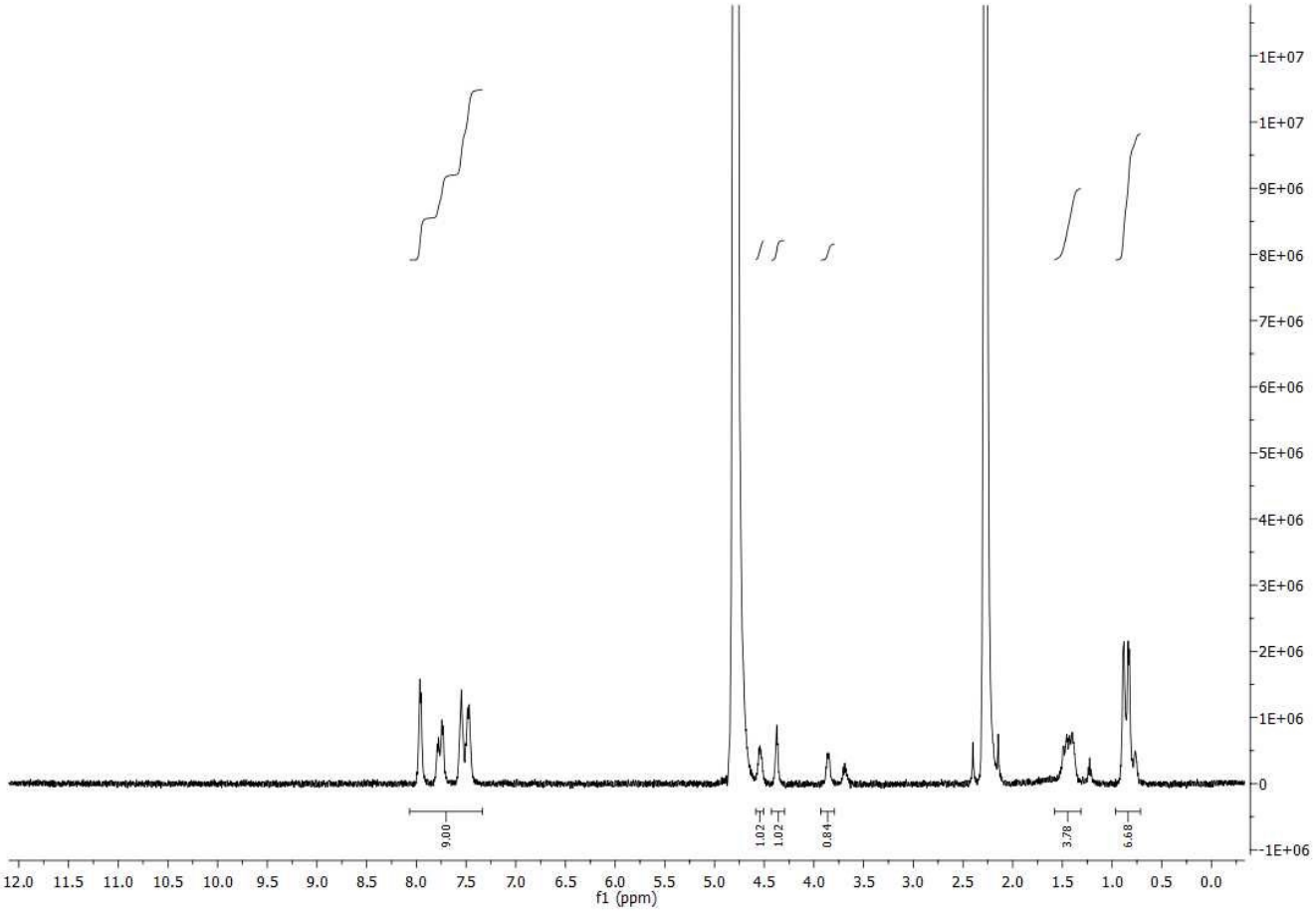

^{1}H NMR spectrum of Fmoc-L (2mg/mL) in D_2O

APPENDIX 3

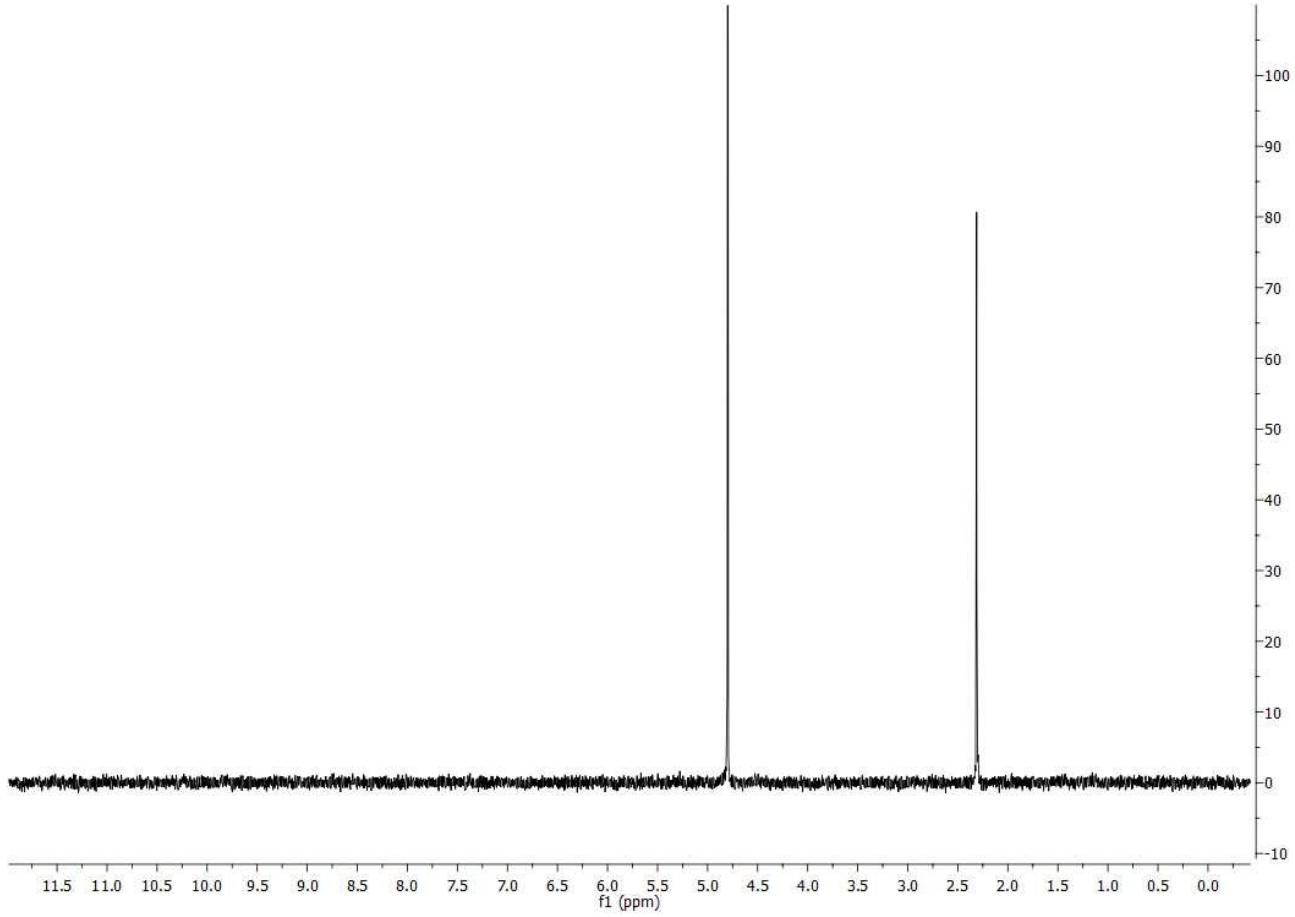

^{1}H NMR spectrum of Fmoc-L (0,36mg/mL) in D_2O